

1 **Application of WRF/Chem over North America under the AQMEII Phase 2: Part II.**
2 **Evaluation of 2010 Application and Responses of Air Quality and Meteorology-Chemistry**
3 **Interactions to Changes in Emissions and Meteorology from 2006 to 2010**

4 Khairunnisa Yahya, Kai Wang, and Yang Zhang*

5 Department of Marine, Earth, and Atmospheric Sciences, NCSU, Raleigh, NC 27695

6 Tadeusz E. Kleindienst

7 National Exposure Research Laboratory, U.S. EPA, Research Triangle Park, NC 27711

8
9 **Abstract**

10 The Weather Research and Forecasting model with Chemistry (WRF/Chem) simulation
11 with the 2005 Carbon Bond gas-phase mechanism coupled to the Modal for Aerosol Dynamics
12 for Europe and the Volatility Basis Set approach for Secondary Organic Aerosol (SOA) are
13 conducted over a domain in North America for 2006 and 2010 as part of the Air Quality Model
14 Evaluation International Initiative (AQMEII) Phase 2 project. Following the Part I paper that
15 focuses on the evaluation of the 2006 simulations, this Part II paper focuses on comparison of
16 model performance in 2006 and 2010 as well as analysis of the responses of air quality and
17 meteorology-chemistry interactions to changes in emissions and meteorology from 2006 to 2010.

18 In general, emissions for gaseous and aerosol species decrease from 2006 to 2010, leading to a
19 reduction in gaseous and aerosol concentrations and associated changes in radiation and cloud
20 variables due to various feedback mechanisms. WRF/Chem is able to reproduce most
21 observations and the observed variation trends from 2006 to 2010, despite its slightly worse
22 performance than WRF that is likely due to inaccurate chemistry feedbacks resulted from less

23 accurate emissions and chemical boundary conditions (BCONs) in 2010. Compared to 2006, the

*Corresponding author. Mailing address: Campus Box 8208, Room 1125, Jordan Hall, 2800 Faucette Drive Raleigh,
NC 27695-8208, USA. Tel: 1-991-515-9688. Fax: 1-919-515-7802. E-mail address: yang_zhang@ncsu.edu

24 performance for most meteorological variables in 2010 gives lower normalized mean biases but
25 higher normalized mean errors and lower correlation coefficients. The model also shows worse
26 performance for most chemical variables in 2010. This could be attributed to underestimations
27 in emissions of some species such as primary organic aerosol in some areas of the U.S. in 2010,
28 and inaccurate chemical BCONs and meteorological predictions. The inclusion of chemical
29 feedbacks in WRF/Chem reduces biases in meteorological predictions in 2010; however, it
30 increases errors and weakens correlations comparing to WRF simulation. Sensitivity simulations
31 show that the net changes in meteorological variables from 2006 to 2010 are mostly influenced
32 by changes in meteorology and those of ozone and fine particulate matter are influenced to a
33 large extent by emissions and/or chemical BCONs and to a lesser extent by changes in
34 meteorology. Using a different set of emissions and/or chemical BCONs help improve the
35 performance of individual variables, although it does not improve the degree of agreement with
36 observed inter-annual trends. These results indicate a need to further improve the accuracy and
37 consistency of emissions and chemical BCONs, the representations of SOA and chemistry-
38 meteorology feedbacks in the online-coupled models.

39 **Keywords:** AQMEII, Emission variation, WRF/Chem, Meteorology-chemistry Interactions,
40 SOA, Air Quality Trends

41

42 **1. Introduction**

43 Changes in meteorology, climate, and emissions affect air quality (e.g., Hogrefe et al.,
44 2004; Leung and Gustafson, 2005; Zhang et al., 2008; Dawson et al., 2009; Gao et al., 2013;
45 Penrod et al., 2014). As federal, state, and local environmental protection agencies enforce the
46 anthropogenic emission control programs, ambient air quality is expected to be continuously

47 improved. However, such an improvement may be compensated by adverse changes in climatic
48 or meteorological conditions (e.g., increases in near surface temperature, solar radiation, and
49 atmospheric stability, or reductions in precipitation) that are directly conducive to the formation
50 and accumulation of air pollutants and that may result in higher biogenic emissions. It is
51 therefore important to examine changes in meteorology/climate and emissions as well as their
52 combined impacts on air quality. The Air Quality Model Evaluation International Initiative
53 (AQMEII) Phase 2 was launched in 2011 to intercompare online-coupled air quality models
54 (AQMs) in their capabilities in reproducing atmospheric observations and simulating air quality
55 and climate interactions in North America (NA) and Europe (EU) (Alapaty et al., 2012). The
56 simulations over NA and EU with multi-models by a number of participants have been
57 performed for two years (2006 and 2010) that have distinct meteorological conditions.
58 Compared with 2006, 2010 is characterized by warmer summer conditions in eastern U.S. and
59 less precipitation over NA (Stoeckenius et al., 2014; Pouliot et al., 2014). In addition, the
60 emissions of key pollutants are reduced in 2010 relative to 2006, e.g., emissions of oxides of
61 nitrogen (NO_x) and sulfur dioxide (SO_2) are reduced by 10-30% and 40-80% for many regions in
62 NA (Pouliot et al., 2014). Comparison of 2010 and 2006 simulations will thus provide an
63 opportunity to examine the success of the emission control programs and the impacts of
64 meteorological/climatic variables on air quality. Compared to model intercomparison during
65 AQMEII Phase 1 (Rao et al., 2012) in which offline-coupled models were used, the use of
66 online-coupled AQMs models during AQMEII Phase 2 allows for study of the interactions
67 between meteorology and chemistry through various direct and indirect feedbacks among
68 aerosols, radiation, clouds, and chemistry (Zhang, 2008; Baklanov et al., 2014). The two year
69 simulations further enable an examination of the responses of air quality and meteorology-

70 chemistry interactions to changes in emissions and meteorology from 2006 to 2010 that was not
71 possible with offline-coupled models.

72 Similar to offline AQMs, large uncertainties exist in online-coupled AQMs, which will
73 affect the model predictions and implications. Such uncertainties lie in the meteorological and
74 chemical inputs such as emissions, initial and boundary conditions (ICONS and BCONs), model
75 representations of atmospheric processes, and model configurations for applications such as
76 horizontal/vertical grid resolutions and nesting techniques. Several studies examined the
77 uncertainties in emissions (e.g., Reid et al., 2005; Zhang et al., 2014) and BCONs (e.g., Hogrefe
78 et al., 2004; Schere et al., 2012). There are also uncertainties in various chemical mechanisms
79 and physical parameterizations used in AQMs such as gas-phase mechanisms (Zhang et al.,
80 2012), aerosol chemistry and microphysical treatments (Zhang et al., 2010), microphysical
81 parameterizations (van Lier-Walqui et al., 2014), convective parameterizations (Yang et al.,
82 2013), boundary layer schemes (Edwards et al., 2006), and land surface models (Jin et al., 2010).
83 Due to the complex relationships in online-coupled AQMs among the emissions, ICONs and
84 BCONs, and model processes that may be subject to inherent limitations, it is difficult to isolate
85 the contributions of model inputs or the representations of atmospheric processes to the model
86 biases. In mechanistic evaluation (also referred to as dynamic evaluation), sensitivity
87 simulations are performed by changing one or a few model inputs or process treatments, while
88 holding others constant. This approach can help diagnose the likely sources of biases in the
89 model predictions.

90 The Weather Research and Forecasting model with Chemistry (WRF/Chem) version
91 3.4.1 with the 2005 Carbon Bond (CB05) gas-phase mechanism coupled with the Modal for
92 Aerosol Dynamics for Europe (MADE) and the Volatility Basis Set (VBS) approach for

93 secondary organic aerosol (SOA) (hereafter WRF/Chem-CB05-MADE/VBS) has been recently
94 developed by Wang et al. (2014). The WRF/Chem-CB05-MADE/VBS has been coupled to the
95 aqueous-phase chemistry scheme (AQChem) based on the AQChem version in CMAQ v5.0 of
96 Sarwar et al. (2011) for both large-scale and convective clouds (Wang et al., 2014). WRF/Chem-
97 CB05-MADE/VBS also contains heterogeneous chemistry involving sulfur dioxide on the
98 surface of aerosols based on Jacob (2000) and treats both aerosol direct and indirect effects. The
99 applications of WRF/Chem-CB05-MADE/VBS to 2006 and 2010 in this work use the same
100 model physical and chemical parameterizations as those in the Part I paper of Yahya et al. (2014)
101 but with different emissions, meteorological ICONs and BCONs, and chemical ICONs and
102 BCONs. The mechanistic evaluation by comparing WRF/Chem-CB05-MADE/VBS predictions
103 for the two years would help understand the sensitivity of the model predictions and performance
104 to different model inputs, and that by comparing WRF/Chem-CB05-MADE/VBS and WRF only
105 predictions would quantify the impacts of chemistry-meteorology feedbacks on the
106 meteorological predictions. A comprehensive evaluation of the 2006 simulation has been
107 presented in the Part I paper of Yahya et al. (2014). In this Part II paper, the differences in
108 emissions, meteorological and chemical ICONs/BCONs, and meteorology between 2010 and
109 2006 are first examined briefly. The model performance in 2010 is then evaluated and compared
110 with that in 2006. Finally, the responses of air quality and meteorology-chemistry interactions to
111 changes in emissions, chemical ICONs/BCONs, and meteorology individually and collectively
112 from 2006 to 2010 are analyzed. The main objectives of this Part II paper are to examine whether
113 the model has the ability to consistently reproduce observations for two separate years, as well as
114 to examine whether the trends in air quality and meteorology-chemistry interactions are
115 consistent for both years. Stoeckenius et al. (2014) carried out an extensive analysis of the trends

116 in emissions and observations of meteorological variables, O₃, SO₂, and PM_{2.5} concentrations
117 between 2006 and 2010. This Part II paper complements the work of Stoeckenius et al. (2014) by
118 examining the changes in WRF/Chem predictions and chemistry-meteorology feedbacks in 2010
119 relative to 2006. Similar evaluations of 2010 and 2006 are performed for the coupled Weather
120 Research and Forecasting – Community Multiscale Air Quality (WRF-CMAQ) system (Hogrefe
121 et al., 2014). Unlike the coupled WRF-CMAQ system used in AQMEII Phase 2 that only
122 simulates aerosol direct effects, WRF/Chem used in this work simulates both aerosol direct and
123 indirect effects. In addition, the work by Hogrefe et al. (2014) involves nudging of temperature,
124 wind speed, water vapor mixing ratio, soil temperature and soil moisture, while the model used
125 for this study did not include any nudging.

126 **2. Differences in Emissions and ICONs/BCONs between 2006 and 2010**

127 **2.1 Emission Trends**

128 The emission variation trends are examined for major precursors for ozone (O₃) and
129 secondary particulate matters (PM) (i.e., sulfur dioxide (SO₂), oxides of nitrogen (NO_x),
130 ammonia (NH₃), volatile organic compounds (VOCs) including both anthropogenic and biogenic
131 VOCs) and primary PM species (elemental carbon (EC) and primary organic aerosol or carbon
132 (POA or POC)). As shown in Table S1, emissions of most species decrease from 2006 to 2010
133 with domainwide averages of -10% to -24%. Comparing to emissions in 2006, the annual
134 emissions of SO₂ and NO_x decrease significantly in 2010, especially at the point sources (Figure
135 S1), with similar variation patterns in all seasons (Figure not shown). The annual emissions of
136 NH₃ decrease over most areas but increase in some areas in California (CA) and Midwest.
137 Unlike the changes in the emissions of SO₂ and NO_x, NH₃ and VOCs emissions exhibit strong
138 seasonal variations in the emission trends, as shown in Figure S2. Although anthropogenic VOC

139 emissions decrease over continental U.S. (CONUS) for all seasons (Figure not shown), the VOC
140 emissions increase in the southeast, which is dominated by enhanced biogenic emissions from
141 vegetation as a response to temperature increases (Stoeckenius et al., 2014). The total annual
142 emissions of EC and POA also decrease but to a smaller extent over most areas of the continental
143 U.S. The changes in annual and seasonal emissions of those species between 2010 and 2006 will
144 affect simulated air quality and meteorology-chemistry interactions. In addition, there exist
145 uncertainties in the NEI emissions. The major sources of uncertainties or errors in the NEI
146 emissions include: (1) the emissions were calculated using a bottom-up approach based on
147 information provided by individual state, local, and tribal air agencies; and (2) improvements in
148 emission-estimation methodology over the years may result in inconsistencies between different
149 years of NEI data (Xing et al., 2013). These will affect the accuracy of the model simulations.

150 **2.2 Differences in Chemical and Meteorological ICONs/BCONs**

151 Large differences exist in the chemical and meteorological ICONs/BCONs used in the
152 simulations. For example, Stoeckenius et al. (2014) reported that the mid-tropospheric seasonal
153 mean O₃ mixing ratios are generally lower by several ppbs in 2010 as compared to 2006,
154 especially during spring and summer. Less Asian mid-tropospheric fine dust was also transported
155 over to the U.S. in the spring of 2010 and less African dust reached the U.S. in the summer of
156 2010 (Stoeckenius et al., 2014). As shown in Figure S3, significant differences exist for January,
157 February, and December (JFD) and June, July, August (JJA) 2010 – 2006 in averaged
158 meteorological ICONs and BCONs of skin temperature and soil moisture fraction 100 to 200 cm
159 below ground extracted from the National Center of Environmental Prediction's (NCEP).

160 **3. Model Performance in 2010 and Its Comparison with 2006**

161 Model predictions in 2010 respond to changes in emissions, BCONs, and meteorology.
162 The model performance for both meteorological and chemical predictions in 2010 is evaluated
163 and compared with that in 2006. The surface observational networks used to evaluate 2010
164 results include the Clean Air Status and Trends Network - CASTNET (rural sites), the
165 Southeastern Aerosol Research and Characterization - SEARCH (southeastern U.S. only, rural
166 and urban sites), the Speciated Trends Network - STN (urban sites), the Interagency Monitoring
167 for Protected Visual Environments - IMPROVE (rural sites), the Air Quality System - AQS
168 (rural and urban sites) and the National Atmospheric Deposition Program - NADP (rural and
169 urban sites). The satellite data used include the Moderate Resolution Imaging Spectroradiometer
170 (MODIS) and TERRA. The Global Precipitation Climatology Center (GPCC) for precipitation is
171 a blend of rain gauge data, satellite data and reanalysis data. Major differences in model
172 performance between the two years and their associations with changes in emissions, BCONs,
173 and meteorology are discussed below.

174 **3.1 Differences in Meteorological Predictions for 2006 and 2010**

175 Table 1 shows the annual mean observed and simulated values as well as correlation
176 coefficients (Corr) between the observed and simulated meteorological variables from the 2010
177 WRF/Chem and WRF simulations. Similar statistics from the 2006 WRF/Chem and WRF
178 simulations can be found in Table 1 in Yahya et al. (2014). Figure 1 shows normalized mean
179 bias (NMB) vs. normalized mean error (NME) plots for several meteorological variables by
180 seasons against several observational networks for 2006 and 2010. In general, there are a number
181 of similar trends in terms of meteorological model performances in 2006 and 2010. These
182 systematic biases give insight into the consistency of the model performance in reproducing
183 observations. First, for T2, the model tends to perform the worst among all seasons for JFD for

184 both 2006 and 2010 and with the exception of JFD 2006 against CASTNET and JJA 2010
185 against CASTNET, the T2 performance falls within an NMB of 0 to ~-10%, which means a
186 slight underprediction of T2 for all other seasons for both years. Second, for SWDOWN, the
187 evaluation against CASTNET gives overpredictions for all seasons for both years with the
188 largest overprediction in JFD and the model performs well against SEARCH with very small
189 positive and negative NMBs for all seasons both years. Third, WS10 is overpredicted for all
190 seasons and for both years against CASTNET and SEARCH. Overall, the correlation
191 coefficients (Corr) for 2006 are better than those of 2010, as the correlations between mean
192 observed and simulated values for all meteorological variables are higher for 2006 compared to
193 2010. However, the biases are smaller for temperature at 2-m (T2) (against CASTNET),
194 downward shortwave radiation (SWDOWN), wind speed at 10-m (WS10), precipitation (Precip)
195 (against NADP), cloud fraction (CF), and cloud droplet number concentrations (CDNC) for 2010
196 compared to 2006. T2 is underpredicted against CASTNET and SEARCH for both 2006 and
197 2010. The seasonal mean NMBs for both 2006 and 2010 (except for JFD 2006) are < 15%, with
198 annual mean NMBs of -7.7% and -4.9%, respectively. With the exception of JFD 2006 against
199 CASTNET, T2 predictions in the other seasons in 2006 for both CASTNET and SEARCH have
200 lower NMEs (< 25%) for 2006. All the seasons in 2010 have an NME of > 25% for T2
201 predictions. For SWDOWN, for both 2006 and 2010, seasonal NMBs range from -10% to 20%
202 with annual mean NMBs of 21.3% and 7.4%, respectively, against CASTNET and 3.0% and
203 12.4%, respectively, against SEARCH; however the seasonal and annual mean NMEs in 2006
204 are < 40% while those in 2010 range from 40% to 65%. Although SWDOWN is overpredicted
205 on an annual basis, T2 is underpredicted in all seasons in 2006 and all seasons except for JJA in
206 2010, as T2 is diagnosed from the skin temperature, which depends on not only SWDOWN but

207 also other variables such as soil properties. The NCEP, Oregon State University, Air Force,
208 National Weather Service Office of Hydrology (NOAH) land surface model used in this case
209 calculates the heat fluxes and skin temperatures based on SWDOWN, the land-use type, and soil
210 properties including soil texture, soil moisture, soil conductivity and thermal diffusivity which
211 vary for different soil types (Chen, 2007). Pleim and Gilliam (2009) also reported the cold bias
212 for T2 especially for the winter of 2006 for their WRF simulations, which was reduced by
213 implementing deep soil temperature and moisture nudging in their work. In this study, however,
214 deep soil data nudging was not used. Annual mean WS10 is overpredicted for both 2006 and
215 2010 (with NMBs of 17.4-27.4% in 2006 and 8-27.5% in 2010) but to a much smaller extent
216 compared to previous studies. This is because the Mass and Owens (2010) surface roughness
217 parameterization is used in this work in WRF and WRF/Chem, which helps reduce typical
218 overpredictions in WS10 overall in both years. SWDOWN tends to be overpredicted for
219 CASTNET due to underpredictions in cloud variables which will be covered in Section 3.4. CF
220 is the only meteorological variable with a better performance in terms of all three measures
221 including Corr, NMB, and NME in 2010 than in 2006 against MODIS. The better performance
222 in CF in 2010 may help reduce annual mean NMBs in CDNC, SWDOWN, and T2 in 2010,
223 although their annual mean NMEs increase and annual mean Corr values decrease.

224 For Precipitation, the model performs consistently well against GPCC for both years with
225 seasonal NMBs within -11% and -12%, and annual NMBs of 0.3% and 1.3%, respectively, for
226 2006 and 2010. The evaluation against NADP shows larger differences with NMBs of 22.2%
227 and 2.5% and Corr values of 0.43 and 0.1 for 2006 and 2010, respectively. As compared to other
228 meteorological variables such as T2, SWDOWN, and WS10, the meteorological performance for
229 precipitation do not follow a clear trend for all seasons or years against NADP and GPCC. For

230 example, precipitation in JJA is underpredicted against NADP and GPCC for 2010 but this is not
231 the case for 2006. In general, the reported biases in precipitation simulated by WRF from
232 literature are significant. For example, Wang and Kotamarthi (2014) studied the precipitation
233 behavior in WRF and showed that even with nudging, the precipitation biases remained up to a
234 root mean square error (RMSE) of 62.5% due to inherent weaknesses in the microphysics and
235 cumulus parameterization schemes. Similarly, WRF/Chem gives large seasonal mean biases (up
236 to 44% in 2006 and up to -26% in 2010) for simulated precipitation for most seasons in 2006 or
237 2010, although the annual mean biases are small to moderate (with NMBs of -2.2% to -1.3% to
238 against GPCC and 9.7-17.6% to against NADP in both years). Yahya et al. (2014) compared and
239 evaluated the full-year WRF and WRF/Chem 2006 simulations with the same physical
240 configurations to analyze the effects of feedbacks from chemistry to meteorology. The results for
241 2006 show that for the evaluation of SWDOWN, T2, and WS10 against CASTNET and
242 SEARCH, the Corr is almost identical for both WRF/Chem and WRF simulations. For
243 evaluation of precipitation against NADP, WRF has a higher Corr compared to WRF/Chem.
244 Unlike 2006, the 2010 WRF only simulation has higher Corr for all meteorological variables
245 compared to the 2010 WRF/Chem simulation except for Precip against GPCC and CF against
246 MODIS. This means that the emissions and chemistry-meteorological feedbacks play an
247 important role in influencing model performance. Section 4.4 will explore this in further detail.
248 Another obvious difference is that the NMBs for the meteorological variables for 2010 are
249 smaller compared to 2006 for all the variables except for Precip against GPCC, while the NMEs
250 are larger for 2010 compared to 2006 for all variables except for Precip against GPCC. A smaller
251 overall averaged NMB but a larger NME may indicate compensation of over- and under-

252 predictions leading to a small bias, but the magnitude of the differences are reflected in the NME
253 values.

254 The same model physics and dynamics options are used for both years. In addition to
255 different emissions, there are characteristic climate differences between the two years that lead to
256 lower Corr and larger NMEs for most meteorological fields in 2010 compared to 2006 for both
257 WRF and WRF/Chem simulations. 2010 is reported to be the warmest year globally since 1895
258 according the National Climactic Data Center (NCDC) (<http://www.ncdc.noaa.gov/cag/>). Even
259 though 2010 has high temperatures compared to previous years, a trend analysis of extreme heat
260 events (EHE) from 1930 to 2010 showed that in 2010, there were more than 35 extreme
261 minimum heat events (where temperatures are extremely low) over southeastern U.S. compared
262 to about ~10 events in 2006. In fact, the number of extreme minimum heat events is the highest
263 overall for CONUS in 2010 compared to all the other years from 1930 onwards (Oswald and
264 Rood, 2014). The Intergovernmental Panel for Climate Change (IPCC) reported that since 1950,
265 weather events have become more extreme likely due to climate change (IPCC, 2012).
266 Grundstein and Dowd (2011) stated that on average, by 2010 there would be 12 more days with
267 extreme apparent temperatures than those in 1949. These studies imply that increased
268 temperatures change the weather in unexpected ways with uncertainties in the state of science
269 (Huber and Gullede, 2011), including models. These high and low temperatures could
270 contribute to the compensation of over- and under-predictions leading to smaller NMBs in
271 general for 2010. To better simulate model extreme heat events, Meir et al. (2013) suggested
272 using a higher spatial resolution with a grid size of 12-km or smaller, better sea surface
273 temperature estimates, and enhanced urbanization parameterization. Gao et al. (2012) reported
274 better results in reproducing extreme weather events with WRF over eastern U.S. at a 4-km × 4-

275 km resolution. In this study, although the urban canopy model is used for both WRF and
276 WRF/Chem simulations, a 36-km × 36-km grid resolution might not be sufficient to reproduce
277 the extreme temperature events (highs and lows) in 2010.

278 As shown in Figure S4, the spatial distribution of MB values for T2 for JFD 2010 by
279 WRF/Chem show very large negative MBs over southeastern U.S. compared to JFD 2006. T2 is
280 also generally underpredicted over southeastern U.S. in both years, but with larger negative
281 biases in 2010 than those in 2006. T2 biases also seem to be more extreme for JFD 2010
282 compared to JFD 2006, with dark red and dark blue colors for the MB markers, indicating large
283 positive and large negative biases, respectively. This could explain the poorer correlation for T2
284 in 2010 compared to 2006 as shown in Table 1. On the other hand, the performances of T2 for
285 JJA 2010 and 2006 are very similar, with MBs ~ -0.1 to 0.1 °C in eastern U.S., large negative
286 MBs at the sites in Montana and Colorado, and a large positive MB at the site in Wyoming.

287 **3.2 Differences in Chemical Predictions for 2006 and 2010**

288 The chemical performance between 2006 and 2010 is more variable compared to the
289 meteorological performance of surface variables. The lower Corr for 2010 compared to 2006 for
290 meteorological variables has a large influence on the model performance for 2010. As shown in
291 Table 1, all the chemical variables for all networks have lower Corr in 2010 compared to 2006.
292 As shown in Figures 2 and 3, maximum 8-hr O₃ concentrations are underpredicted to a larger
293 extent in 2010 compared to 2006, dominating the O₃ annual performance in 2010. These results
294 are consistent with the results of Hogrefe et al. (2014). The large underpredictions of maximum
295 8-hr O₃ in JFD 2010 over southeastern U.S. are attributed to larger cold biases in T2 shown in
296 Figure S4 and reduced NO_x and VOC emissions in 2010 relative to their levels in 2006. While
297 reduced NO_x levels can result in an increase in nighttime O₃ concentrations due to reduced NO_x

298 titration of O₃, the impact of reduced NO_x titration on the maximum 8-hr O₃ is small. As shown
299 in Figure S4, the temperature biases for both years are relatively similar. Over northeastern U.S.,
300 the T2 bias is generally less than -0.1 °C for JJA in both years. However, as shown in Figure 2,
301 O₃ concentrations over northeastern U.S. in JJA 2010 have negative biases whereas those over
302 northeastern U.S. in JJA 2006 have positive biases. In this case, emissions might play a
303 significant role in the underprediction of O₃ concentrations over northeastern U.S. in JJA 2010.
304 Hourly average surface NO_x emissions decrease significantly over northeastern U.S. in JJA from
305 2006 to 2010. As shown in Figure 3, 2006 model performance for O₃ is generally good for all
306 seasons and all networks.

307 According to Table 1 and Figure 1, WRF/Chem predicts SWDOWN to a lower extent in
308 2010 compared to 2006 against CASTNET. Khiem et al. (2010) reported that during the
309 summer, a large percentage of the variations in peak O₃ concentrations during the summer can be
310 attributed to changes in seasonally averaged daily maximum temperature and seasonally
311 averaged WS10. Simulated WS10 is lower for 2010 compared to 2006 in general; therefore,
312 WS10 does not seem to contribute to reduced O₃ concentrations (through dispersion, increased
313 dry deposition) in 2010. Figure 4 shows diurnal variations of observed and simulated
314 WRF/Chem T2 and O₃ concentrations from CASTNET in JJA 2006 and 2010. The diurnal
315 averaging provides insight whether the underpredictions of O₃ mixing ratios is a systematic bias
316 during the daytime or nighttime or both. The diurnally averaged observed temperatures show a
317 similar trend in JJA 2006 to 2010 against T2 measurements from CASTNET. This shows that the
318 model is able to reproduce T2 for different years. The temperature trends also correlate strongly
319 with the O₃ trends. At night, where the model has cold bias, O₃ concentrations are underpredicted
320 to a larger extent. The O₃ concentrations show a larger underprediction for JJA 2010 compared

321 to JJA 2006. The underpredictions in O₃ in both 2006 and 2010 can be explained by several
322 reasons. For example, Im et al. (2014) showed that MACC underpredicts O₃ mixing ratios,
323 particularly in winter and spring during both day and night and in summer and fall during
324 nighttime. As indicated by Wang et al. (2014) and Makar et al. (2014), the inclusion of aerosol
325 indirect effects also tends to reduce O₃ mixing ratios, comparing to the models that simulate
326 aerosol direct effect only or do not simulate aerosol direct and indirect effects (i.e., offline-
327 coupled models).

328 Figure 5 shows spatial distribution of NMBs for PM_{2.5} concentrations for JFD and JJA
329 2006 and 2010 against IMPROVE, STN, and SEARCH. Overall, JJA 2006 and JJA 2010 have
330 similar spatial distribution patterns of NMBs for all sites over CONUS except for several sites in
331 northwestern U.S. where PM_{2.5} concentrations are underpredicted for JJA 2010 but overpredicted
332 for JJA 2006. However, many sites have positive NMBs over eastern and central U.S. for JFD
333 2006, whereas more sites have negative NMBs over eastern and central U.S. for JFD 2010.
334 Statistics from Yahya et al. (2014) and Table 1 show that in general, the simulated
335 concentrations of PM_{2.5} and all PM_{2.5} species decrease from 2006 to 2010, however, the Corr
336 values for PM_{2.5} and PM_{2.5} species become worse in 2010 compared to 2006. As shown in Figure
337 6, PM_{2.5} concentrations for 2006 can be overpredicted or underpredicted, depending on seasons
338 and networks, with an equal distribution of positive and negative NMBs. However for 2010,
339 PM_{2.5} concentrations tend to be underpredicted for all seasons and for all networks except for
340 JFD against SEARCH. As shown in Figure 7, NMBs for PM_{2.5} species for 2006 at individual
341 monitoring sites range from -40% to 60%, while those for 2010 range from -80% to 80%. The
342 markers are more spread out covering a wider range of NMBs and NMEs for 2010 with more
343 extremes as compared to the markers for 2006 clustered around the zero NMB line. NMEs for

344 PM_{2.5} species in 2006 remain below 100%. NO₃⁻ concentrations are slightly underpredicted in
345 2006 against all networks; however, NO₃⁻ levels in 2010 are largely underpredicted, likely due to
346 the large decrease in NO_x emissions from 2006 to 2010 and the increase in T2. The NMBs for
347 IMPROVE and SEARCH OC remain low from 2006 to 2010; however, the NMEs increase
348 significantly. For TC against IMPROVE, the NMB and NME in 2010 are larger in magnitudes in
349 2010 than those in 2006. SO₄²⁻ has lower NMBs but higher NMEs for all networks in 2010
350 compared to 2006. EC concentrations are generally overpredicted in 2006 for all networks but
351 underpredicted against SEARCH and largely overpredicted against IMPROVE in 2010. NH₄⁺
352 also has higher NMEs in 2010 compared to 2006. Overall, the evaluation in 2010 shows larger
353 NMEs and weaker correlations for all PM_{2.5} species compared to 2006.

354 Figure 8 shows the time series plots for 24-hr average concentrations of PM_{2.5}, SO₄²⁻ and
355 NO₃⁻ against STN for 2006 and 2010. In 2006, the daily-average PM data were collected on a
356 daily basis in 2006 but every 3 days in 2010. The model is able to predict most of the observed
357 peaks and troughs for 2006 even though the observed and simulated magnitudes are significantly
358 different for several days. For 2010, the model does not show large spikes and can reproduce the
359 magnitudes well, although it does not predict the peaks and troughs as well as 2006 for some
360 months (e.g., Jan-March and July-Sept. for PM_{2.5}). This could be attributed in part to the weaker
361 correlations of meteorological variables in 2010 compared to 2006. For example, inaccurate
362 predictions of WS10 can influence the transport and dry deposition of aerosols. An
363 overprediction of precipitation increases the wet deposition of aerosols. Poor predictions of T2
364 can influence the planetary boundary layer height (PBLH) and both can also affect the
365 distribution of aerosol concentrations. NO₃⁻ concentrations for the winter months are moderately
366 underpredicted in 2006 but largely underpredicted in 2010, likely due to the underpredictions in

367 nitrogen dioxide (NO₂) concentrations (Yahya et al., 2014). Section 4 will discuss in further
368 detail the role of emissions, meteorology and chemical ICONs/BCONs on O₃ and PM_{2.5}
369 concentrations.

370 **3.3 SOA Evaluation for 2006 and 2010**

371 The VBS framework in WRF/Chem of Ahmadov et al. (2012) provides a more realistic
372 treatment of SOA compared to previous SOA treatments such as the 2-product model by Odum
373 et al. (1996) used in the Secondary Organic Aerosol Model (SORGAM) of Schell et al. (2001).
374 Wang et al. (2014) evaluated SOA and OC concentrations simulated from WRF/Chem-CB05-
375 MADE/VBS and WRF/Chem-CB05-MADE/SORGAM over NA for July 2006 against field
376 campaign data from Offenberg et al. (2011) at the Research Triangle Park (RTP), NC for July
377 2006. They showed significant improvement in simulating SOA and total organic aerosol (TOA)
378 by VBS than by SORGAM. In this study, SOA and OC predictions are evaluated against
379 available field campaign data at RTP, NC in eastern U.S. from Offenberg et al. (2011) for 2006
380 only, and Pasadena, CA and Bakersfield, CA in western U.S. from Lewandowski et al. (2013)
381 for 2010 only (note that no observations are available at the same sites for both years). The RTP
382 site is located in a semi-rural area. Pasadena, CA is located about 11 miles from downtown Los
383 Angeles (LA), and Bakersfield, CA is located about ~100 miles from downtown LA. Both sites
384 are classified as urban/industrial sites. OC concentrations were measured using an automated,
385 semicontinuous elemental carbon-organic carbon (EC-OC) instrument. The observed SOA
386 masses were determined from organic tracers extracted from filter samples (Lewandowski et al.,
387 2013). Simulated OC concentration is calculated by summing up SOA and POA, and dividing
388 the total OA by 1.4 (Aitken et al., 2008).

389 As shown in Figures 9 and S5, the model overpredicts SOA but underpredicts OC at RTP
390 in 2006, because (1) the SOA formed from alkanes and alkenes is excluded in the observations
391 from RTP but simulated in WRF/Chem, and (2) WRF/Chem may have overestimated the aging
392 rate coefficient for both anthropogenic and biogenic surrogate VOC precursors (Wang et al.
393 (2014)). The SOA overprediction due to those reasons compensates the underprediction in SOA
394 due to omission of SOA from POA, leading to a net SOA overprediction at RTP in 2006. By
395 contrast, the VBS underpredicts SOA in 2010 with NMBs of -55.3% and -75.3% at Bakersfield
396 and Pasadena, respectively, which is mainly due to the omission of SOA formation from POA in
397 the current VBS-SOA module in this version of WRF/Chem. As shown in Figure S6, SOA to OC
398 ratios at RTP in 2006 are in the range of 50-80%, whereas they are < 20% at Bakersfield, CA
399 and < 40% Pasadena, CA in 2010. This indicates that neglecting SOA formation from POA
400 would have much larger impact on SOA predictions at the two CA sites in 2010 than at RTP in
401 2006, due to the dominance of POA in TOA at the two CA sites. As shown in Figure 9, the
402 model underpredicts OC at RTP in 2006 and significantly underpredicts OC at the two sites in
403 CA in 2010. The differences in OC performance in both years are caused by different locations
404 (i.e., RTP in 2006 and the two CA sites in 2010) that have different ratios of POC to OC as
405 mentioned previously. OC performance thus largely depends on SOA performance at RTP but
406 on POA performance at the two sites in CA. This is why the OC performance remains poor
407 despite a relatively good performance in SOA at the two sites in CA. Worse OC performance
408 over the two CA sites in 2010 may also indicate potentially large underestimation of POA
409 emissions over the western U.S.

410 **3.4 Differences in Aerosol-Cloud Predictions for 2006 and 2010**

411 Figure 10 shows NMBs vs. NMEs of several aerosol and cloud variables for JFD and JJA
412 in 2006 and 2010 against satellite data. Table 1 lists the corresponding annual performance
413 statistics for 2010. The model is able to reproduce generally similar performances against
414 observations for most of the aerosol-cloud variables for both 2006 and 2010 as the trends of
415 NMBs and NMEs are quite similar for both seasons in both years. For JJA 2006 and 2010, all
416 cloud variables are underpredicted with approximately the same magnitudes of NMBs and
417 NMEs. For JJA, the model performs better for 2010 for CF, aerosol optical depth (AOD), and
418 cloud optical thickness (COT) in terms of seasonal mean spatial distribution. For JFD, the model
419 performs better for CF and cloud water path (CWP) in 2010. In terms of annual statistics,
420 compared to 2006, 2010 has lower NMBs for CF and COT but larger biases in AOD, CWP, and
421 cloud condensation nuclei (CCN), leading to large differences in aerosol-radiation and cloud –
422 radiation feedbacks, which in turn affect the performance of meteorological and chemical
423 predictions. Despite the differences in model performance of meteorological and chemical
424 variables in 2010 compared to 2006, performance of cloud variables do not vary significantly.
425 One possible reason is because the evaluation of aerosol-cloud variables is based on monthly
426 values that are averaged out on a seasonal basis. The meteorological and chemical variables
427 shown earlier are evaluated based on site-specific, and hourly, daily, or weekly data.

428 **3.5 Differences in Observed and Simulated Trends between 2010 and 2006**

429 Table 2 shows the percentage changes in observed and WRF only and WRF/Chem
430 simulated variables between 2010 and 2006. Overall, the model is able to predict the trends in all
431 major meteorological, chemical, and aerosol-cloud-radiation variables between 2006 and 2010
432 with a few exceptions (e.g., WS10 against CASTNET, Precip, CF, maximum 8-hr O₃ against
433 CASTNET, and 24-hr EC against IMPROVE). The trends in simulated T2, SWDOWN, and

434 SEARCH WS10 are generally consistent with the observed trends from 2006 to 2010. Both
435 observed and simulated temperatures at 2-m (T2) at the CASTNET sites increase by ~4 °C or
436 ~35 to 40% from 2006 to 2010. For downward shortwave radiation (SWDOWN), both observed
437 and simulated values at the CASTNET and SEARCH sites increase by ~1 to 3% and by ~5 to
438 7%, respectively, from 2006 to 2010. The observed WS10 remains relatively constant at
439 CASTNET in both years. The simulated WS10 by WRF also shows no change but that by
440 WRF/Chem shows a small decrease (by -8.3%) for the CASTNET sites. Comparing to a
441 SEARCH observed change of ~-4% in WS10, WRF and WRF/Chem predict a larger decrease
442 from 2006 to 2010 (~-12 to -13%). The trends for Precip and CF for simulated variables are not
443 consistent with observed trends from 2006 to 2010. Observed NADP Precip increased slightly
444 from 2006 to 2010 by ~7%, however both simulated WRF and WRF/Chem show a small
445 decrease from 2006 to 2010. Observed mean GPCP Precip remained relatively constant from
446 2006 to 2010, however, WRF only shows a slight increase (~4%) while WRF/Chem shows a
447 larger decrease (-12%) from 2006 to 2010. MODIS CF decreased by -0.2% from 2006 to 2010
448 whereas both WRF and WRF/Chem show small increases ~3-4% from 2006 to 2010. Apart from
449 the large biases in the evaluation of precipitation, the decrease in precipitation is likely due to the
450 smaller decrease in SWDOWN for WRF/Chem compared to observations between 2006 and
451 2010. This would result in less convective precipitation during the summer but increased CF for
452 2010. In addition, PM_{2.5} is underpredicted but agrees better with observed PM_{2.5} in 2010 than in
453 2006. Underpredicted PM_{2.5} concentrations will also affect the formation of clouds and
454 precipitation via various direct and indirect effects.

455 The simulated decreasing trends between 2006 and 2010 are overall consistent with the
456 observed decreasing trend between 2006 and 2010 for all species except for maximum 8-hr O₃

457 concentrations from CASTNET and EC from IMPROVE. CASTNET maximum 1-hr and 8-hr
458 O₃ concentrations change very little from 2006 to 2010 whereas WRF/Chem shows a moderate
459 decrease of 14-15%. The large decrease in simulated O₃ mixing ratios in 2010 can be attributed
460 to a large decrease in O₃ mixing ratios from the ICONs and BCONs (Stoeckenius et al., 2014).
461 The IMPROVE observed EC concentrations decreased by ~22% from 2006 to 2010, however,
462 WRF/Chem shows a small increase (by ~2%). For PM_{2.5} concentrations, the simulated decrease
463 from 2006 to 2010 by WRF/Chem is larger than the observed decrease for both STN and
464 IMPROVE. Similar steeper decreases by WRF/Chem also occur for SO₄²⁻ against STN, NO₃⁻
465 against IMPROVE, TC against STN, and OC against IMPROVE likely due to the influence of
466 ICONs/BCONs and emissions.

467 **4. Responses of 2010 Predictions to Changes in Emissions and Meteorology**

468 The changes in emissions, boundary conditions, and meteorology between 2010 and 2006
469 lead to changes in simulated air quality and the chemistry-meteorology feedbacks, which in turn
470 change meteorological and air quality predictions during the next time step.

471 **4.1 Air Quality Predictions**

472 Simulated air quality responds nonlinearly to the changes in emissions. Figures 11, S7-
473 S9 show the seasonal changes between 2010 and 2006 in ambient mixing ratios of gases (SO₂,
474 NO₂, NH₃, O₃, and hydroxyl - OH) and concentrations of PM species (SO₄²⁻, NO₃⁻, NH₄⁺,
475 organic matter or OM, EC, POA, anthropogenic SOA or ASOA, biogenic SOA or BSOA, and
476 PM_{2.5}). SO₂ and NO₂ concentrations tend to decrease for all seasons at most locations over
477 CONUS due to the decrease in their emissions. The increases in NO₂ concentrations over urban
478 areas in eastern U.S. in March, April, May (MAM) in 2010 relative to 2006 could be due to a
479 few reasons including decreased photolytic conversion from NO₂ to NO due to a decrease in

480 SWDOWN and less NO_2 conversion to nitric acid (HNO_3) due to decreased OH concentrations.
481 The NO_2 hot spots also correlate to the decrease in hourly O_3 concentrations in urban areas. This
482 could indicate an increased titration of nighttime O_3 by NO. This is an important result for policy
483 implications, as reducing NO_x emissions may reduce NO_2 concentrations overall for CONUS,
484 but may not reduce NO_2 concentrations in several areas, especially in urban areas due to a
485 combination of titration and complex interplay with local meteorology. NH_3 mixing ratios
486 generally decrease in the U.S., except over eastern U.S. in MAM and September, October, and
487 November (SON), where there are increases. NH_3 emissions decrease, however, over eastern
488 U.S. in all seasons. The increase in NH_3 concentrations in MAM and SON could be attributed to
489 a number of reasons including less NH_3 conversion to NH_4^+ to neutralize SO_4^{2-} and NO_3^- and less
490 dispersion of NH_3 concentrations due to decreased wind speeds over eastern and southeastern
491 U.S. in MAM and SON, respectively, in 2010 compared to 2006. In JJA and SON, high OM
492 concentrations in Canada are attributed to the enhanced impacts of BCONs by increasingly
493 convergent flow in this region. OM is made up of both POA and SOA. An increase in VOC
494 emissions in eastern U.S. in MAM and SON leads to increases in OM concentrations. Decreases
495 in VOC emissions in western U.S. for all seasons lead to decreases in OM concentrations. The
496 OM concentrations in some areas, however, do not follow a linear relationship with VOC
497 emissions, such as southeastern U.S. in JJA, where VOC emissions increase from 2006 to 2010
498 but OM concentrations decrease. A decrease in POA concentrations must dominate the overall
499 decrease in OM concentrations, even under increased temperatures and biogenic VOC emissions
500 in this area. $\text{PM}_{2.5}$ concentrations decrease for all seasons and most regions of the CONUS,
501 which is attributed mainly to decreases in precursor gases, especially the inorganic precursors
502 SO_2 and NO_x in eastern U.S. Increased $\text{PM}_{2.5}$ concentrations in JFD and MAM in the Midwest

503 are due to surface temperature decreases, dominating in this region (Stoeckenius et al., 2014).
504 This in turn leads to increased particle nitrate concentrations (Campbell et al., 2014).

505 **4.2 Meteorological Predictions**

506 Figure S10 compares the seasonal changes between 2010 and 2006 in several
507 meteorological variables that affect air pollution including SWDOWN, T2, WS10, PBLH, and
508 Precip simulated by WRF only simulations without considering chemistry feedbacks. Large
509 changes occur in those variables between the two years, e.g., 10-50 $W m^{-2}$ increases in
510 SWDOWN in western and Midwest in JJA, generally warmer in JJA and SON over most areas
511 but cooler by 3-10 °C in eastern U.S. in JFD, and with reduced Precip in eastern or southeastern
512 U.S. in JJA and SON but increased Precip in northwestern U.S. in MAM and JJA and in western
513 U.S. in JFD. ICONs and BCONs for skin temperatures shown in Figure S3 greatly influence T2
514 shown in Figure S10 for JFD and JJA.

515 Figures 12 and S11 show the seasonal changes between 2010 and 2006 in several
516 meteorological and cloud variables (SWDOWN, T2, WS10, Precip, PBLH, AOD, COT, CF,
517 CWP, and CDNC) for WRF/Chem that accounts for meteorology-chemistry feedbacks. The
518 relationships between various meteorological variables have been discussed in Yahya et al.
519 (2014). Comparing to the differences in predictions of SWDOWN, T2, WS10, Precip, and PBLH
520 between 2010 and 2006 WRF only simulation shown in Figure S10 and WRF/Chem simulations
521 shown in Figures 12 and S11, the differences in those meteorological variables do not vary
522 significantly in terms of trends of average seasonal spatial distributions between 2010 and 2006
523 WRF simulations and between 2010 and 2006 WRF/Chem simulations. However, there are
524 differences in magnitudes, especially for SWDOWN. SWDOWN is affected most by the
525 addition of chemistry in WRF/Chem as compared to WRF, especially for JFD through indirect

526 feedback of clouds on radiation. As shown in Figure 12, the decrease in SWDOWN from 2006 to
527 2010 is larger over north-central and north-western U.S. and the increase in SWDOWN is
528 smaller over north-eastern and southwestern U.S. for MAM (WRF/Chem) compared to MAM
529 (WRF). For SON, the increase in SWDOWN from 2006 to 2010 simulated by WRF/Chem is
530 larger over eastern U.S. than that by WRF. The differences between WRF and WRF/Chem are
531 the largest for SWDOWN over northeastern U.S. in JFD with an increase in SWDOWN
532 simulated by WRF but a decrease simulated by WRF/Chem from 2006 to 2010. The differences
533 in SWDOWN are likely due to the differences in CF between the two sets of simulation pairs, as
534 the spatial distribution for CF is consistent with that of SWDOWN. As expected, there are slight
535 differences between T2 and PBLH between WRF and WRF/Chem (2010 – 2006) due to changes
536 in radiation. There are also small differences between precipitation between WRF and
537 WRF/Chem. The aerosol-cloud-radiation feedbacks due to the differences between WRF and
538 WRF/Chem for 2010 will be discussed in Section 4.3.

539 The increase in SWDOWN from 2006 to 2010 does not necessarily translate to an
540 increase in T2. However, in general, increases in SWDOWN lead to increase in T2, as shown in
541 SON in Figure 12, where SWDOWN generally increases over most of the continental U.S., T2
542 also increases over most of CONUS. In general, the largest differences in T2 between 2006 and
543 2010 occur in SON (increase) and JFD (decrease). The decrease in T2 in JFD in north-central
544 U.S. and parts of Canada is significant as it results in a decrease in WS10 and PBLH. For JJA,
545 there is an obvious pattern between SWDOWN and Precip, with an increase in SWDOWN
546 corresponding to a decrease in Precip and vice versa. According to IPCC (2007), in the warm
547 seasons over land, strong negative correlations dominate as increased sunshine results in less

548 evaporative cooling. Figure S12 compares wind vectors superposed with T2 in 2006 and 2010
549 from WRF/Chem and shows the largest differences are in JJA.

550 As expected, the spatial pattern of SWDOWN changes is anti-correlated with CF changes
551 for all seasons between 2006 and 2010; however, the changes in the spatial pattern of CF do not
552 correlate with changes in CDNC. CF in each grid cell is set to either 0 (no clouds), or to 1
553 (cloudy) if total cloud water + ice mixing ratio $> 1 \times 10^{-6} \text{ kg kg}^{-1}$ (Wu and Zhang, 2005). In this
554 study, the monthly CF is then normalized over the total number of time steps and vertical layers,
555 giving a value of CF between 0 and 1 in each grid cell. In contrast, the calculations of CDNC in
556 the model depend on the supersaturation, aerosol concentrations, aerosol hygroscopicity and
557 updraft velocity (Abdul-Razzak and Ghan, 2004). The changes in CF are controlled by large
558 scale state variables including temperature and relative humidity, while CDNC depends on more
559 complex changes in microphysical variables. The dominant CDNC decrease in MAM, JJA, and
560 SON, is due to lower $\text{PM}_{2.5}$ concentrations, which in turn lower the effective number of cloud
561 condensation nuclei. However, exception occurs in southeast U.S. where $\text{PM}_{2.5}$ decreases but
562 CDNC increases. This is because CDNC also depends on other variables including the amount of
563 liquid water in the atmosphere. The cloud liquid water path over southeastern U.S. increases,
564 which may explain the increase in CDNC. The spatial pattern for precipitation correlates to that
565 of CF. The spatial pattern of CWP also corresponds to a certain extent with CF. PBLH increases
566 when the ground warms up during the day and decreases when the ground cools so PBLH might
567 be intuitively related to SWDOWN and T2. However, this consistent trend is now obvious in the
568 plots, because the simulated growth of the planetary boundary layer (PBL) also depends on the
569 surface sensible latent and heat fluxes and the entrainment of warmer air from the free
570 troposphere (Chen, 2007).

571 **4.3 Meteorology-Chemistry Feedback Predictions**

572 As shown in Table 1, similar to 2006, comparison of the performance of most
573 meteorological variables between WRF/Chem and WRF for 2010 is improved in terms of NMBs
574 when chemistry-meteorology feedbacks are included. This indicates the importance and benefits
575 of inclusion of such feedbacks in online-coupled models. However, unlike 2006 for which both
576 WRF only and WRF/Chem simulations show similar values of Corrs and NMEs, the 2010 WRF
577 simulations give higher Corr and lower NMEs than the 2010 WRF/Chem simulations. This
578 indicates the impact of worse chemical predictions on chemistry-meteorology feedbacks that can
579 in turn affect meteorological predictions. These results indicate the needs of further improvement
580 of the online-coupled models in their representations of chemistry-meteorology feedbacks.
581 Yahya et al. (2014) analyzed differences in meteorological performance between WRF/Chem
582 and WRF for 2006. Figure S13 shows absolute seasonal differences between the meteorological
583 predictions from WRF/Chem and WRF for 2010. The differences between WRF/Chem and
584 WRF are consistent for both 2006 and 2010. SWDOWN in general is higher for WRF/Chem
585 compared to WRF for all seasons, with larger differences over the eastern portion of the domain
586 compared to the western portion. Other obvious similarities between 2006 and 2010 include the
587 increase in T2 over the northern portion of the domain for MAM, SON and JFD; increase in
588 PBLH over the ocean in the eastern part of the domain for all seasons; and increases over the
589 ocean for CF for all seasons. The reasons for the differences between WRF/Chem and WRF in
590 terms of meteorological variables have been discussed in Yahya et al. (2014).

591 **4.4 Sensitivity Simulations**

592 The aforementioned differences in WRF/Chem predictions between 2006 and 2010 are
593 caused by changes in emissions, meteorology, and meteorological and chemical ICONs/BCONs.

594 Additional sensitivity simulations for the months of January and July 2010 are carried out to
595 estimate the individual contributions of each of those changes to the total net changes in model
596 predictions. Table 3 summarizes the configurations of the sensitivity simulations. The 2006
597 baseline simulations are designated as Run 1, the 2010 baseline simulations are designated as
598 Run 2, and the two sensitivity simulations are designated as Runs 3 and 4. Run 3 is the
599 sensitivity simulation using 2006 emissions but keeping all other inputs (e.g., meteorology and
600 chemical ICONs/BCONs) and model configurations the same as Run 2. Run 4 is the sensitivity
601 simulation using 2006 emissions and chemical ICONs/BCONs keeping all other inputs and
602 model configurations the same as Run 2. Figures 13 and 14 show the changes due to combined
603 effects of emissions, meteorological and chemical ICONs/BCONs (Run 2 - Run 1 in column 1),
604 changes due to the changes in emissions (Run 2 - Run 3 in column 2), changes due to the
605 changes in chemical ICONs/BCONs (Run 3 - Run 4 in column 3), and changes due to the
606 changes in meteorology including ICONs/BCONs (Run 4 - Run 1 in column 4) for January and
607 July, respectively. Since the impact of ICONs is only important at the beginning of the
608 simulations whereas the impact of BCONs persists throughout the simulations, the changes due
609 to changes in chemical BCONs will dominate over those due to changes chemical
610 ICONs/BCONs.

611 Both Figures 13 and 14 show that the differences in the meteorology due to the impact of
612 meteorological ICONs/BCONs generated by WRF/Chem contribute to the largest differences in
613 T2 and SWDOWN for both months (columns 1 and 4). For comparison, the changes in emissions
614 and chemical ICONs/BCONs lead to less significant differences in T2 and SWDOWN (columns
615 2 and 3). The overall decrease in emissions from 2006 to 2010 results in a slight increase in both
616 T2 and SWDOWN in January (column 2 in Figure 13), and a larger increase in SWDOWN in

617 July (column 2 in Figure 14) due to decreases in aerosol loading. There is a small decrease in T2
618 and SWDOWN in January (column 3 in Figure 13) due to influences of chemical
619 ICONs/BCONs used for both years, but a larger decrease occurs in SWDOWN in July (column 3
620 in Figure 14). As shown in Figures 13 and 14 (column 1), changes in O₃ are influenced by all
621 factors and the overall change of O₃ mixing ratio is a combination of changes in emissions,
622 meteorological and chemical ICONs/BCONs. The O₃ mixing ratios are greatly increased due to
623 the use of 2010 emissions as compared to 2006 emissions (column 2 in Figure 13), indicating
624 that using a different set of emissions can produce an increase of up to a domain mean of 6 ppb.
625 Conversely, O₃ mixing ratios are greatly decreased (with a reduction of a domain mean of 6 ppb)
626 due to the use of the 2010 chemical ICONs/BCONs compared to the 2006 chemical
627 ICONs/BCONs (column 3 in Figure 13). The use of different meteorological ICONs/BCONs
628 also results in varying degrees of changes of O₃ mixing ratios domainwide as O₃ mixing ratios
629 are influenced by photolysis and other meteorological parameters including wind and PBLH
630 (column 4 in Figure 13). In addition, T2 and SWDOWN influence the amount of BVOC
631 emissions produced, which also in turn influences O₃ mixing ratios. In VOC-limited urban
632 centers over eastern U.S. (Campbell et al., 2014), a small increase in radiation or T2 will increase
633 BVOC emissions, increasing O₃ mixing ratios, and vice versa. In July (Figure 14), the decrease
634 in O₃ mixing ratios between 2006 and 2010 (column 1) is largely influenced by chemical
635 ICONs/BCONs (column 3) and to a smaller extent by meteorological ICONs/BCONs (column
636 4). In this case, the difference in emissions (column 2) does not seem to significantly impact the
637 changes of O₃ mixing ratios between July 2006 and 2010 (column 1). For January (Figure 13),
638 PM_{2.5} concentrations decrease due to decreasing emissions and chemical ICONs/BCONs
639 (columns 2 and 3). However, the use of 2010 meteorological ICONs/BCONs results in an

640 increase in $PM_{2.5}$ concentrations over most of the domain except for the northeastern U.S. (with a
641 domain mean increase of $0.4 \mu\text{g m}^{-3}$) (column 4). The overall differences (column 1 in Figure
642 13) are mainly due to net effects of emissions (column 2) and changes in meteorology (column
643 4). For $PM_{2.5}$ in July (Figure 14), the net changes from 2006 and 2010 (column 1) are dominated
644 entirely by changes in emissions (column 2) that increase in the southeastern and central U.S. but
645 decrease in the remaining domain, even though meteorological ICONs/BCONs also play a
646 significant role (column 4).

647 Table S2 in the supplementary material shows the statistics NMB, NME, and Corr for a
648 number of variables for the sensitivity simulations for January and July. The statistics in bold
649 highlights the sensitivity simulations with the best performance (i.e. with the lowest NMB and
650 NME and the highest Corr). The WRF/Chem performance of T2 against CASTNET improves to
651 a large extent in terms of NME and Corr for Runs 3 and 4 (especially for January when Run 2
652 performs poorly), which use 2006 emissions. This indicates that at least for January (and to a
653 smaller extent for July), the inaccuracy of emissions may have contributed to the worse
654 performance of T2 against CASTNET. Run 3 also gives the best performance of T2 against
655 CASTNET, which indicates that improvement in both emissions and chemical ICONs/BCONs
656 can improve meteorological performances for both January and July. For SWDOWN, Runs 3
657 and 4 improve the performance against CASTNET for January (with lower NMB and NME and
658 higher Corr). The cloud-aerosol variables are affected to a smaller extent by changes in
659 emissions and chemical ICONs/BCONs compared to the meteorological variables. The
660 performance for CF remains relatively the same for January and July. The performance for COT
661 and AOD improves slightly for January with a lower NMB and NME but becomes worse in July
662 with a higher NMB and NME. However, as the performance of meteorological variables is

663 significantly different, a small change in cloud-aerosol variable can lead to a large change in
664 meteorological variables. The performances for O₃ and PM_{2.5} concentrations in January and July
665 improve to a large extent when using 2006 emissions and especially when 2006 chemical
666 ICONs/BCONs are also used. The higher emissions of NO_x, VOCs, and CO for July 2006
667 compared to 2010 contribute to the better O₃ performance, and the higher emissions of primary
668 SO₄²⁻, NO₃⁻, EC and OA for 2006 contribute to the better PM_{2.5} performance for Run 3 in July.
669 However for January, a combination for both 2006 emissions and chemical ICONs/BCONs
670 improve the O₃ performance, while PM_{2.5} performance is the best using 2010 emissions and
671 2010 ICONs/BCONs. This indicates that inaccuracies in emissions and chemical ICONs/BCONs
672 in 2010, especially in January could contribute to the poor performance of WRF/Chem in 2010.
673 These will, in turn affect the meteorological performance to a large extent.

674 To evaluate if the sensitivity simulations with different meteorology, emissions, and
675 chemical ICs/BCs for January and July 2010 can improve the model's capability in reproducing
676 the trends in both meteorological and chemical variables, compared to baseline results in 2006
677 and 2010, the absolute and percentage differences between the monthly mean of observations of
678 major variables in 2010 and 2006 and between simulation results from three simulation pairs:
679 Runs 2 and 1, Runs 3 and 1, and Runs 4 and 1 are calculated and summarized in Table 4. The
680 differences between 2010 baseline simulation and the 2006 baseline simulations (Run 2 – Run 1)
681 show the impact of all the changes (including emissions, meteorology, and chemical ICs/BCs) in
682 the 2010 simulation relative to the 2006 simulation on the simulated variation trends and the
683 degree of agreement in the variation trends calculated from the two baseline simulations with the
684 observed changes. Comparisons of differences between Run 3 and Run 1 (Run 3 – Run 1) with
685 those between Run 2 and Run 1 (Run 2 – Run 1) and between Run 4 and Run 1 (Run 4 – Run 1)

686 with those between Run 2 and Run 1 (Run 2 – Run 1) indicate the impact of changes in
687 emissions and meteorology, respectively, on the simulated variation trends and their degree of
688 agreement with the observed changes.. As shown in Table 4, the baseline model simulations
689 (Run 2 – Run 1)are not able to reproduce the trends in terms of either the signs or magnitude or
690 both in the observations for some variables, including SWDOWN against CASTNET, COT
691 against MODIS, maximum 8-hr O₃ against CASTNET, and PM_{2.5} against STN in January and
692 CF against MODIS in July. Changing the emissions (Run 3 – Run 1) does not improve the
693 variation trends from 2006 to 2010 with the exception of SWDOWN against CASTNET in
694 January and maximum 8-hr O₃ against CASTNET in July. Changing the meteorology (Run 4 –
695 Run 1) also does not improve the variation trends to a large extent with the exception of
696 maximum 8-hr O₃ against CASTNET in January and SWDOWN against CASTNET in July. In
697 fact, Run 2 – Run 1 (which are the baseline simulations) overall performs the closest to the
698 observed trends of major variables for January and July 2006 to 2010.

699

700 **5. Summary and Conclusions**

701 This study compares model performance in 2010 and 2006 and examines the changes in
702 emissions, boundary conditions, and meteorology, as well as the responses of meteorology, air
703 quality and chemistry-meteorology feedbacks to those changes collectively and individually
704 between 2010 and 2006. In general, the emissions of most gaseous and aerosol species over
705 CONUS decrease from 2006 to 2010 with the exception of NH₃ emissions over several areas in
706 JFD and biogenic VOCs mainly over eastern U.S. in JJA and SON. The increases in biogenic
707 VOCs are caused by increases in temperatures in 2010 in eastern U.S. during these seasons.
708 Overall, T2 increases from 2006 to 2010, however, the changes of T2 and other meteorological

709 variables including SWDOWN, WS10, PBLH, and Precip vary spatially over CONUS with the
710 largest differences for SWDOWN. The reduced emissions and changed meteorology result in
711 decreased concentrations in general for gaseous and aerosol species except for species influenced
712 by high BCONs, e.g., for OM concentrations over Canada in MAM and JJA. Due to increases in
713 biogenic emissions, OM concentrations increase over eastern U.S. CDNC generally decreases
714 over the U.S. due to the decreases in $PM_{2.5}$ concentrations and CCN from 2006 to 2010. The
715 spatial distributions of other meteorological and cloud variables are consistent with known
716 processes, e.g., SWDOWN is high and precipitation is low where CF is low. There is no clear
717 spatial correlation between CF and CDNC due to the differences in their inherent prognostic
718 treatments. COT corresponds relatively well to AOD, especially for JJA in both years. CWP
719 also corresponds well to COT. Sensitivity simulations show that the net changes in
720 meteorological predictions in 2010 relative to 2006 are influenced mostly by changes in
721 meteorology. Those of O_3 and $PM_{2.5}$ concentrations are influenced to a large extent by emissions
722 and/or chemical ICONs/BCON, but meteorology may also influence them to some degrees,
723 particularly in winter.

724 In general, the model performs well in terms of Corr and NMEs for almost all
725 meteorological and chemical variables in 2006 but not as well in 2010 despite lower NMBs for
726 most variables in 2010, due mainly to inaccuracies in emission estimates and chemical BCONs
727 and ICONs used for 2010 simulations. The model is able to reproduce the observations to a large
728 extent for most meteorological surface variables. The model performs relatively well for $PM_{2.5}$
729 concentrations. However, OC concentrations are significantly underpredicted against field data
730 for 2010 in Bakersfield and Pasadena, CA, due mainly to underestimations in emissions of POA
731 that contributes to most OC and also in part to underestimations in emissions of gaseous

732 precursors of SOA and inaccurate meteorological predictions in 2010. The model also has
733 significant biases for a few aerosol-cloud-radiation variables except for CF and QVAPOR,
734 however, the model is able to reproduce the trends in aerosol-cloud-radiation variables for 2006
735 and 2010. The variation trends for most meteorological and chemical variables simulated by
736 WRF and WRF/Chem are overall consistent with the observed trends from 2006 to 2010 but for
737 2010, WRF/Chem performs slightly worse than WRF. Similar to 2006, the inclusion of
738 chemistry-meteorology feedbacks reduces NMBs for most meteorological variables in 2010,
739 although WRF gives higher Corr and lower NMEs than WRF/Chem.

740 A number of sensitivity simulations are also conducted for January and July 2006 and
741 2010 to quantify the relative impact of emissions, chemical ICONs/BCONs, and meteorology on
742 model performance of major meteorological and chemical species as well as on the variation
743 trends between 2006 and 2010. Using more accurate emissions and chemical and meteorological
744 ICONs/BCONs will help improve the performance of some individual chemical and
745 meteorological surface variables. Although the 2006 emissions may not represent the true
746 emissions for 2010, the 2010 sensitivity simulations using the 2006 emissions show improved
747 model performance. However, using 2006 emissions for 2010 simulations does not improve the
748 degree of agreement with observed inter-annual trends as the consistency between the 2006 and
749 2010 emissions are affected between the simulations. The baseline simulations for 2006 and
750 2010 reproduce the observed trends the best as a consistent set of 2006 and 2010 emissions are
751 used. The current 2006 and 2010 emissions were developed taking into account the inter-annual
752 trends, the improvement of emissions need to be carried out consistently for all individual
753 simulation years when simulating multi-year cases.

754 WRF/Chem with CB05-MADE/VBS option used in this work has been incorporated into
755 the WRF/Chem version 3.6.1 to be released in version 3.7 of WRF-Chem (available for
756 download from <http://www.mmm.ucar.edu/wrf/users/>). The results in this work indicate a need
757 to further improve the accuracy of emissions and chemical BCONs, and the representations of
758 organic aerosols and chemistry-meteorology feedbacks in WRF/Chem. In addition, the
759 improvements in aerosol-cloud treatments such as the aerosol activation parameterization, and in
760 the microphysics and cumulus parameterizations that affect the formation of precipitation are
761 needed to improve the model's capability in reproducing the state of the atmosphere and also
762 inter-annual trends. While the long-term air quality simulations using WRF/Chem with aerosol-
763 cloud-radiation feedbacks in this work can provide guidance on future model development and
764 improvement, they do not provide the impact of those feedback mechanisms on the model
765 performance. Quantifying such impacts requires another set of simulations using a version of
766 WRF/Chem that does not treat aerosol direct and indirect effects, which is not yet available to
767 public. The simulations with and without aerosol direct and indirect effects have indeed been
768 performed by Makar et al. (2014a, b) using a different model that was specially designed to
769 quantify such impacts. It would be useful to develop a version of WRF/Chem that does not treat
770 aerosol direct and indirect effects for this impact assessment. In particular, comparison of the
771 episodic or long-term simulation results using WRF/Chem that includes and excludes feedback
772 mechanisms against observations of aerosol and cloud variables can provide further insight into
773 whether inclusion of those aerosol direct and indirect effects can improve the model's capability
774 in reproducing observations. Those simulations should be considered when the version of
775 WRF/Chem without aerosol direct and indirect effects and computer resources become available.
776

777 **Acknowledgements**

778 This study is funded by the National Science Foundation EaSM program (AGS-1049200)
779 at NCSU. The following agencies have prepared the datasets used in this study: the U.S. EPA
780 (North American emissions processing), Environment Canada, Mexican Secretariat of the
781 Environment and Natural Resources (Secretaría del Medio Ambiente y Recursos Naturales,
782 SEMARNAT) and National Institute of Ecology (Instituto Nacional de Ecología) (North
783 American national emissions inventories), the European Center for Medium Range Weather
784 Forecasting Global and Regional Earth-system (Atmosphere) Monitoring using Satellite and in-
785 situ data (ECMWF/GEMS) project and Meteo France/Centre national de recherches
786 météorologiques (CNRM-GAME) for the Monitoring Atmospheric Composition and Climate
787 (MACC) IC/BCs. Meteorological IC/BCs are provided by the National Center for Environmental
788 Protection. Ambient North American concentration measurements are provided by several U.S.
789 networks (AQS, CASTNET, IMPROVE, SEARCH, and STN). North American precipitation-
790 chemistry measurements are provided by several U.S. networks (CASTNET, and NADP). GPCP
791 Precipitation data is provided by the National Oceanic and Atmospheric Administration's Earth
792 System Research Laboratory in the Physical Sciences Division (NOAA/OAR/ESRL PSD),
793 Boulder, Colorado, USA, from their web site at <http://www.esrl.noaa.gov/psd/>. 2006 and 2010
794 SOA/OC data at RTP, NC, Bakersfield, CA and Pasadena, CA were provided by John Offenberg,
795 U.S. EPA. Cloud variables were provided by MODIS. We thank Georg Grell, NOAA, Christian
796 Hogrefe, U.S. EPA, Paul Makar, Environment Canada, Christoph Knote, NCAR, and Patrick
797 Campbell, NCSU, for helpful discussions on inputs and outputs of AQMEII model
798 intercomparison. We would also like to acknowledge high-performance computing support from
799 Yellowstone by NCAR's Computational and Information Systems Laboratory, sponsored by the

800 National Science Foundation. This work also used the Stampede Extreme Science and
801 Engineering Discovery Environment (XSEDE) high-performance computing support which is
802 supported by the National Science Foundation grant number ACI-1053575.

803 The US Environmental Protection Agency through its Office of Research and
804 Development collaborated in the research described here. The manuscript has been subjected to
805 external peer review and has not been cleared for publication. Mention of trade names or
806 commercial products does not constitute endorsement or recommendation for use.

807 **References**

808 Abdul-Razzak, H., and Ghan, S.J.: A parameterization of aerosol activation, 2. Multiple
809 aerosol types, *J. Geophys. Res.*, 105, 5, 6837-6844, 2000.

810 Ahmadov, R., McKeen, S.A., Robinson, A.L., Bahreini, R., Middlebrook, A.M., de Gouw, J.A.,
811 Meagher, J., Hsie, E.-Y., Edgerton, E., Shaw, S., and Trainer, M.: A volatility basis set model
812 for summertime secondary organic aerosols over the eastern United States in 2006, *J.*
813 *Geophys. Res.*, 117, D06301, doi:10.1029/2011JD016831, 2012.

814 Aitken, A.C., Decarlo, P.F., Kroll, J.H., Worsnop, D.R., Huffman, J.A., Docherty, K.S., Ulbrich,
815 I.M., Mohr, C., Kimmel, J.R., Sueper, D., Sun, Y., Zhang, Q., Trimborn, A., Northway, M.,
816 Ziemann, P.J., Canagaratna, M.R., Onasch, T.B., Alfarra, M.R., Prevot, A.S.H., Dommen, J.,
817 Duplissy, J., Metzger, A., Baltensperger, U., and Jimenez, J.L.: O/C and OM/OC ratios of
818 primary, secondary and ambient organic aerosols with high-resolution time-of-flight aerosol
819 mass spectrometry, *Environ. Sci. Technol.*, 42, 4478-4485, 2008.

820 Alapaty, K.V., Mathur, R., Pleim, J.E., Hogrefe, C., Rao, S.T., Ramaswamy, V., Galmarini, S.,
821 Schapp, M., Vautard, R., Makar, P., Baklanov, A., Kallos, G., Vogel, B., and Sokhi, R.: New

822 Directions: Understanding interactions of air quality and climate change at regional scales,
823 Atmos. Environ., 49, 3, doi:10.1016/j.atmos.env.2011.12.016, 2012.

824 Baklanov, A., Schlunzen, K., Suppan, P., Baldasano, J., Brunner, D., Aksoyoglu, S., Carmichael,
825 G., Douros, J., Flemming, J., Forkel, R., Galmarini, S., Gauss, M., Grell, G., Hirtl, M., Joffre,
826 S., Jorba, O., Kaas, E., Kaasik, M., Kallos, G., Kong, X., Korsholm, U., Kurganskiy, A.,
827 Kushta, J., Lohmann, U., Mahura, A., Manders-Groot, A., Maurizi, A., Moussiopoulous,, N.,
828 Rao, S.T., Savage, N., Seigneur, C., Sokhi, R.S., Solazzo, E., Solomos, S., Sorensen, B.,
829 Tsegas, G., Vignati, E., Vogel, B and Zhang, Y.: Online Coupled Regional Meteorology-
830 Chemistry Models in Europe: Current Status and Prospects, Atmos. Chem. Phys., 14, 317-
831 398, doi:10.5194/acp-14-317-2014, 2014.

832 Campbell, P., Zhang, Y., Yahya, K., Wang, K., Hogrefe, C., Pouliot, G., Knote, C., Hodzic, A.,
833 San Jose, R., Perez, J.L., Guerrero, P.J., Baro, R., and Makar, P.: A Multi-Model Assessment
834 for the 2006 and 2010 Simulations under the Air Quality Model Evaluation International
835 Initiative (AQMEII) Phase 2 over North America, Part I. Indicators of the Sensitivity of O₃
836 and PM_{2.5} Formation to Precursor Gases, Atmos. Environ.,
837 doi:10.1016/j.atmosenv.2014.12.026, 2014.

838 Chen, F.: The Noah Land Surface Model in WRF, A short tutorial, NCAR LSM group meeting,
839 Boulder, CO, 17 April 2007, 2007.

840 Dawson, J. P., Racherla, P. N., Lynn, B. H., Adams, P. J., and Pandis, S. N.: Impacts of climate
841 change on regional and urban air quality in the eastern United States: Role of meteorology. J.
842 Geophys. Res., 114, D05308, doi:10.1029/2008JD00984, 2009.

843 Edwards, J.M., Beare, R.J., and Lapworth, A.J.: Simulation of the observed evening transition
844 and nocturnal boundary layers: single column modeling, *Q.J.R. Meteorol. Soc.*, 132, 61 – 80,
845 2006.

846 EPA: National Emission Inventory – Ammonia emissions from animal husbandry operations,
847 Draft Report, January 30, available at :
848 http://www.epa.gov/ttnchie1/ap42/ch09/related/nh3inventorydraft_jan2004.pdf, 2014.

849 Gao, Y., Fu, J.S., Drake, J.B., Liu, Y., and Lamarque, J.-F.: Projected changed of extreme
850 weather events in the eastern United States based on a high resolution climate modeling
851 system, *Environ. Res. Lett.*, 7, 044025, 2012.

852 Gao, Y., Fu, J. S., Drake, J. B., Lamarque, J. F., and Liu, Y.: The impact of emission
853 and climate change on ozone in the United States under representative concentration
854 pathways (RCPs), *Atmos. Chem. Phys.*, 13, 9607–9621, doi:10.5194/acp-13-9607-2013,
855 2013.

856 Grundstein, A., and Dowd, J.: Trends in extreme apparent temperatures over the United States,
857 1949-2010, *J. Appl. Meteor. Climatol.*, 50, 1650-1653, 2011.

858 Hogrefe, C., Lynn, B., Civerolo, K., Ku, J.-Y., Rosenthal, J., Rosenzweig, C., Goldberg, R.,
859 Gaffin, S., Knowlton, K., and Kinney, P.L.: Simulating changes in regional air pollution over
860 the eastern United States due to changes in global and regional climate and emissions, *J.*
861 *Geophys. Res.*, 109, doi: 10.1029/2004JD004690, 2004.

862 Hogrefe, C., Pouliot, G., Wong, D., Torian, A., Roselle, S., Pleim, J., and Mathur, R.: Annual
863 application and evaluation of the online coupled WRF-CMAQ system over North America
864 under AQMEII Phase 2, *Atmos. Environ.*, doi:10.1016/j.atmosenv.2014.12.034, 2014.

865 Hong, S., Lakshmi, V., Small, E.E., Chen, F., Tewari, M., and Manning, K.W.: Effects of
866 vegetation and soil moisture on the simulated land surface processes from the coupled
867 WRF/Noah model., *J. Geophys. Res.*, 114, D18, doi:10.1029/2008JD011249, 2009.

868 Huber, D.G., and Gullede.: Extreme weather and climate change: Understanding the link and
869 managing the risk, Center for Climate and Energy Solutions, available at :
870 <http://www.c2es.org/publications/extreme-weather-and-climate-change>, 2011.

871 IPCC: Climate change 2007: the physical science basis. In: Solomon, S., Qin, D., Manning, M.
872 (Eds.), Contribution of Working Group I to the Fourth Assessment Report of the
873 Intergovernmental Panel on Climate Change, 2007.

874 IPCC: Managing the risks of extreme events and disasters to advance climate change adaptation
875 (SREX), A special report of Working Groups I and II of the Intergovernmental Panel on
876 Climate Change, [Field, C.B., V. Barros, T.F. Stocker, D. Qin, D.J. Dokken, K.L. Ebi, M.D.
877 Mastrandrea, K.J. Mach, G.-K., Plattner, S.K. Allen, M. Tignor, and P.M. Midgley (eds.),
878 Cambridge University Press, Cambridge, UK, and New York, NY, USA, 582 pp., 2012.

879 Im, et al.: Evaluation of operational on-line-coupled regional air quality models over Europe and
880 North America in the context of AQMEII phase 2. Part 1: Ozone, *Atmos. Environ.*, doi:
881 10.1016/j.atmosenv.2014.09.042, 2014.

882 Jacob, D.: Heterogeneous chemistry and tropospheric ozone, *Atmos. Environ.*, 34, 2131 – 2159,
883 2000.

884 Jimenez, P., Parra, R., and Baldasano, J.M.: Influence of initial and boundary conditions for
885 ozone modeling in very complex terrains: A case study in the northeastern Iberian Peninsula,
886 *Environ. Mod. Software*, 22, 1294-1306, 2007.

887 Jin, J., Miller, N.M., and Schlegel, N.: Sensitivity study of four land surface schemes in the WRF
888 model, *Adv. Met.*, 2010, doi: 10.1155/2010/167436, 2010.

889 Khiem, M., Ooka, R., Huang, H., Hayami, H., Yoshikado, H., and Kawamoto, Y.: Analysis of
890 the relationship between changes in meteorological conditions and the variation in summer
891 ozone levels over the central Kanto area, *Adv. Met.*, 2010, doi:10.1155/2010/349248, 2010.

892 Leung, L., and Gustafson, W.: Potential regional climate change and implications to US air
893 quality, *Geophys. Res. Lett.*, 32, 16, L16711, doi:10.1029/2005GL022911, 2005.

894 Lewandowski, M., Piletic, I.R., Kleindienst, T.E., Offenber, J.H., Beaver, M.R., Jaoui, M.,
895 Docherty, K.S., and Edney, E.O.: Secondary organic aerosol characterization at field sites
896 across the United States during the spring-summer period, *Intern. J. Environ. Anal. Chem.*,
897 2013, 2013.

898 Makar, P. et al., Feedbacks between air pollution and weather, part 2: Effects on chemistry,
899 *Atmos. Environ.*, doi:10.1016/j.atmosenv.2014.10.021, 2014.

900 Mass, C., and Owens, D.: WRF Model Physics: Progress, problems and perhaps some solutions,
901 Presented at the 11th WRF Users' Workshop, Boulder, CO, 21 – 25 June 2010, 2010.

902 Meir, T., Orton, P.M., Pullen, J., Holt, T., Thompson, W.T., and Arend, M.F.: Forecasting the
903 New York City urban heat island and sea breeze during extreme heat events, *Wea.*
904 *Forecasting*, 28, 1460-1477, 2013.

905 Odum, J.R., Hoffmann, T., Bowman, F., Collins, D., Flagan, R.C., and Seinfeld, J.H.:
906 Gas/Particle partitioning and secondary organic aerosol yields, *Environ. Sci. Tech.*, 30, 2580-
907 2585, 1996.

908 Offenberg, J.H., Lewandowski, M., Jaoui, M., and Kleindienst, T.E.: Contributions of biogenic
909 and anthropogenic hydrocarbons to secondary organic aerosol during 2006 in Research
910 Triangle Park, NC, *Aero. Air Qual. Res.*, 11, 99 – 108, 2011.

911 Oswald, E.M., and Rood, R.B.: A trend analysis of the 1930-2010 extreme heat events in the
912 continental United States, *J. Appl. Meteor. Climatol.*, 53, 565-582, 2014.

913 Penrod, A., Y. Zhang, K. Wang, S.-Y. Wu, and Leung, R.L.: Impacts of Future
914 Climate and Emission Changes on U.S. Air Quality, *Atmos. Environ.*, 89, 533-547, 2014.

915 Pleim, J.E., and Gilliam, R.: An Indirect Data Assimilation Scheme for Deep Soil Temperature
916 in the Pleim-Xiu Land Surface Model, *J. Appl. Meteor. Climatol.*, 48, 1362 – 1376, 2009,
917 doi:10.1175/2009JAMC2053.1.

918 Pouliot, G., van der Gon, H.D., Kuenen, J., Makar, P., Zhang, J., and Moran, M.: Analysis of the
919 Emission Inventories and Model-Ready Emission Datasets of Europe and North America for
920 Phase 2 of the AQMEII Project, *Atmos. Environ.*, doi:10.1016/j.atmosenv.2014.10.061,
921 2014.

922 Rao, S., S. Galmarini, and Steyn, D.G.: AQMEII: An International Initiative for the
923 Evaluation of Regional-Scale Air Quality Models-Phase 1, *Atmos. Environ.*, Special Issue,
924 53, 1 – 224, 2012.

925 Reid, J.S., Koppmann, R., Eck, T.F., and Eleuterio, D.P.: A review of biomass burning emissions
926 part II: intensive physical properties of biomass burning particles, *Atmos. Chem. Phys.*, 5,
927 799 – 825, 2005.

928 Samaali, M., Moran, M.D., Bouchet, V.S., Pavlovic, R., Cousineau, S., and Sassi, M.: On the
929 influence of chemical initial and boundary conditions on annual regional air quality model
930 simulations for North America, *Atmos. Environ.*, 43, 32, 4873-4885, 2009.

931 Sarwar, G., Fahey, K., Napelenok, S., Roselle, S., and Mathur, R.: Examining the impact of
932 CMAQ model updates on aerosol sulfate predictions, 10th Annual CMAQ Models-3 Users's
933 Conference, Chapel Hill, NC, 2011.

934 Schell, B., Ackermann, I.J., Hass, H., Binkowski, F.S., and Ebel, A.: Modeling the formation of
935 secondary organic aerosol within a comprehensive air quality model system, *J. Geophys.*
936 *Res.*, 106, 28275 – 28293, 2001.

937 Schere, K., Flemming, J., Vautard, R., Chemel, Colette, A., Hogrefe, C., Bessagnet, B., Meleux,
938 F., Mathur, R., Roselle, S., Hu, R.-M., Sokhi, R.S., Rao, S.T., Galmarini, S.: Trace
939 gas/aerosol boundary concentrations and their impacts on continental-scale AQMEII
940 modeling domains, *Atmos. Environ.*, 53, 38-50, 2012.

941 Stoeckenius, T., Chemel, C., Zagunis, J., and Sakulyanontvittaya, T.: A Comparison between
942 2010 and 2006 Air Quality and Meteorological Conditions, and Emissions and Boundary
943 Conditions for the AQMEII-2 North American Domain, *Atmos. Environ.*, in review, 2014.

944 Van Lier-Walqui, M., Vukicevic, T., and Posselt, D.J.: Linearization of microphysical
945 parameterization uncertainty using multiplicative process perturbation parameters, *Mon.*
946 *Wea. Rev.*, 142, 401 – 413, 2014.

947 Wang, J., and Kotamarthi, V.R.: Downscaling with a nested regional climate model in near-
948 surface fields over the contiguous United States, *J. Geophys. Res. Atmos.*, 119, 14, 2014,
949 doi:10.1002/2014JD021696.

950 Wang, K., K. Yahya, Y. Zhang, S.-Y. Wu, and G. Grell.: Implementation and Initial Application
951 of A New Chemistry-Aerosol Option in WRF/Chem for Simulation of Secondary Organic
952 Aerosols and Aerosol Indirect Effects, *Atmos. Environ.*,
953 doi:10.1016/j.atmosenv.2014.12.007, 2014.

954 Wu, J., and Zhang, M.: Simulations of clouds and sensitivity study by Weather Research and
955 Forecast Model for Atmospheric Radiation Measurement case 4, Fifteenth Arm Science
956 Team Meeting Proceedings, 14 – 18 Mar 2005, Daytona Beach, FL, 2005.

957 Xing, J., Pleim, J., Mathur, R., Pouliot, G., Hogrefe, C., Gan, C.-M., and Wei, C.: Historical
958 gaseous and primary aerosol emissions in the United States from 1990 to 2010, *Atmos.*
959 *Chem. Phys.*, 13, 7531 – 7549, 2013, doi:10.5194/acp-13-7531-2013.

960 Yahya, K., Wang, K., Gudoshava, M., Glotfelty, T., and Zhang, Y.: Application of WRF/Chem
961 over the continental U.S. under the AQMEII Phase II: Comprehensive Evaluation of 2006
962 Simulation, *Atmos. Environ.*, doi:10.1016/j.atmosenv.2014.08.063, 2014.

963 Yang, B., Qian, Y., Lin, G., Leung, L.R., Rasch, P.J., Zhang, G.J., McFarlane, S.A., Zhao, C.,
964 Zhang, Y., Wang, H., Wang, M., and Liu, X.: Uncertainty quantification and parameter
965 running in the CAM5 Zhang-McFarlane convection scheme and impact of improved
966 convection on the global circulation and climate, *J. Geophys. Res.*, 118, 395 – 415, 2013.

967 Zhang, Y.: Online-coupled meteorology and chemistry models: history, current status, and
968 outlook, *Atmos. Chem. Phys.*, 8, 2895-2932, 2008.

969 Zhang, Y., Hu, X., Leung, L. R., and Gustafson Jr., W.I.: Impacts of regional climate change on
970 biogenic emissions and air quality, *J. Geophys. Res.* 113, D18310,
971 doi:10.1029/2008JD009965, 2008.

972 Zhang Y., X.-Y. Wen, and Jang C.J.:, Simulating chemistry-aerosol-cloud-radiation-climate
973 feedbacks over the continental U.S. using the online-coupled Weather Research Forecasting
974 Model with chemistry (WRF/Chem), *Atmos. Environ.*, 44, 3568-3582, 2010.

975 Zhang, Y., Chen, Y.-C., Sarwar, G., and Schere, K.: Impact of Gas-Phase Mechanisms on
976 Weather Research Forecasting Model with Chemistry (WRF/Chem) Predictions:

977 Mechanism Implementation and Comparative Evaluation, *J. Geophys. Res.*, 117, D1,
978 doi:10.1029/2011JD015775, 2012.

979 Zhang, Y., Wang, W., Wu, S.-Y., Wang, K., Minoura, H., and Wang, Z.-F.: Impacts of Updated
980 Emission Inventories on Source Apportionment of Fine Particle and Ozone over the
981 Southeastern U.S., *Atmos. Environ.*, 588, 133-154, 2014.

982

983 **Table 1. Annual performance statistics for 2010 Predictions of WRF and WRF/Chem**

Network or Site name	Variable	WRF					WRF/Chem				
		Mean Obs	Mean Sim	Corr	NMB (%)	NME (%)	Mean Obs	Mean Sim	Corr	NMB (%)	NME (%)
CASTNET	T2	15.9	15.0	0.93	-5.0	15.8	15.9	15.1	0.64	-4.9	32.9
SEARCH	T2	19.4	18.4	0.94	-4.3	12.3	19.4	18.4	0.65	-5.1	27.6
CASTNET	SWDOWN	176.1	214.7	0.91	21.8	36.2	176.1	189.2	0.80	7.4	50.4
SEARCH	SWDOWN	217.7	245.0	0.91	11.5	31.6	217.7	211.0	0.78	-3.0	47.2
CASTNET	WS10	2.3	3.0	0.44	28.1	66.4	2.3	3.0	0.17	27.5	80.7
SEARCH	WS10	2.2	2.4	0.47	9.6	50.9	2.2	2.4	0.23	8.0	62.3
NADP	Precip	18.9	20.7	0.54	10.2	71.2	18.9	20.5	0.55	9.7	70.6
GPCC	Precip	2.2	2.3	0.83	1.1	22.6	2.2	2.2	0.83	-1.3	22.0
MODIS	CF	57.6	60.4	0.82	6.2	12.7	57.6	57.8	0.87	0.3	8.9
MODIS	AOD	-	-	-	-	-	0.10	0.05	-0.09	-46.6	54.4
MODIS	COT	-	-	-	-	-	17.2	6.3	0.45	-63.5	63.6
MODIS	CWP	-	-	-	-	-	160.1	97.3	0.54	-39.2	54.9
MODIS	QVAPOR	-	-	-	-	-	1.04	1.13	0.96	9.0	27.7
MODIS	CCN	-	-	-	-	-	0.33	0.09	0.60	-73.2	73.2
TERRA	CDNC	-	-	-	-	-	155.0	123.5	0.10	-20.0	59.2
CASTNET	Max 1-h O ₃	-	-	-	-	-	47.4	33.2	0.40	-30.0	34.8
CASTNET	Max 8-h O ₃	-	-	-	-	-	43.8	32.7	0.40	-25.3	32.0
AQS	Max 1-h O ₃	-	-	-	-	-	48.4	40.7	0.34	-15.8	28.0
AQS	Max 8-h O ₃	-	-	-	-	-	42.3	35.3	0.20	-17.0	29.2
STN	24-h PM _{2.5}	-	-	-	-	-	11.0	9.7	0.17	-11.5	54.6
IMPROVE	24-h PM _{2.5}	-	-	-	-	-	4.5	4.0	0.44	-11.5	56.0
STN	24-h SO ₄	-	-	-	-	-	2.2	2.6	0.33	19.0	68.5
IMPROVE	24-h SO ₄	-	-	-	-	-	1.0	1.3	0.50	21.1	72.3
STN	24-h NO ₃	-	-	-	-	-	1.4	0.7	0.10	-45.6	89.1
IMPROVE	24-h NO ₃	-	-	-	-	-	0.4	0.2	0.30	-43.3	95.5
STN	24-h NH ₄	-	-	-	-	-	1.0	1.0	0.21	1.5	72.5
STN	24-h EC	-	-	-	-	-	0.4	1.0	0.14	147.1	179.5
IMPROVE	24-h EC	-	-	-	-	-	0.2	0.3	0.29	78.5	123.8
STN	24-h TC	-	-	-	-	-	2.8	2.5	0.10	-11.9	62.0
IMPROVE	24-h OC	-	-	-	-	-	0.9	0.6	0.18	-29.6	74.2
IMPROVE	24-h TC	-	-	-	-	-	1.0	0.9	0.21	-11.8	72.8
Pasadena, CA ²	SOA	-	-	-	-	-	0.63	0.16	0.1	-75.3	78.3
Bakersfield, CA ²	SOA	-	-	-	-	-	0.51	0.23	0.3	-55.3	65.9

984
985
986
987
988
989
990
991
992
993

¹ Units are as follows: SWDOWN (W m⁻²), GLW (W m⁻²), OLR (W m⁻²), T2 (°C), RH2 (%), WS10 (m s⁻¹), WD10 (°), Precip (mm), CWP (g m⁻²), QVAPOR (cm), CCN (10⁹ cm⁻²), CDNC (cm⁻²), O₃ (ppb), PM and PM species (µg m⁻³). CASTNET - the Clean Air Status and Trends Network; AQS – the Aerometric Information Retrieval System Air Quality System; SEARCH - the Southeastern Aerosol Research and Characterization; GPCC - the Global Precipitation Climatology Centre; MODIS - the Moderate Resolution Imaging Spectroradiometer; IMPROVE – the Interagency Monitoring for Protected Visual Environmental; STN – the Speciated Trends Network. Note that IMPROVE did not contain NH4+ data for 2010. “-” indicates that the results of those variables not available from the WRF only simulation.

² The observed SOA data are taken from Lewandowski et al. (2013).

995 **Table 2. Percentage changes in observed and simulated variables between 2010 and 2006**

Network or Site name	Variable	Obs	WRF	WRF/Chem
CASTNET	T2	35.7	38.6	40.1
SEARCH	T2	1.3	0.0	0.5
CASTNET	SWDOWN	2.1	2.6	1.4
SEARCH	SWDOWN	7.3	7.4	5.2
CASTNET	WS10	0.0	0.0	-8.3
SEARCH	WS10	-4.3	-13.4	-12.4
NADP	Precip	6.7	-4.3	-1.5
GPCC	Precip	0.0	4.5	-12.0
MODIS	CF	-0.2	3.7	3.0
MODIS	AOD	-28.6	-	-44.4
MODIS	COT	4.2	-	6.8
MODIS	CWP	-10.2	-	-11.1
MODIS	QVAPOR	-47.5	-	-42.1
MODIS	CCN	-2.9	-	-30.8
CASTNET	Max 1-h O ₃	-0.5	-	-15.0
CASTNET	Max 8-h O ₃	0.6	-	-13.9
AQS	Max 1-h O ₃	-3.9	-	-14.6
AQS	Max 8-h O ₃	-4.9	-	-17.4
STN	24-h PM _{2.5}	-9.9	-	-20.8
IMPROVE	24-h PM _{2.5}	-16.1	-	-27.0
STN	24-h SO ₄	-25.8	-	-33.3
IMPROVE	24-h SO ₄	-23.7	-	-26.3
STN	24-h NO ₃	-11.3	-	-27.8
IMPROVE	24-h NO ₃	-20.0	-	-53.5
STN	24-h NH ₄	-25.3	-	-31.9
STN	24-h EC	-39.5	-	-1.6
IMPROVE	24-h EC	-21.6	-	2.4
STN	24-h TC	-38.1	-	-24.2
IMPROVE	24-h OC	-17.3	-	-45.5
IMPROVE	24-h TC	-25.5	-	-35.7

996

997

998

999

1000

1001

1002

1003

1004

¹The percentages are calculated according to this formula: [(2010 value – 2006 value) /2006 value] * 100%.
 CASTNET - the Clean Air Status and Trends Network; AQS – the Aerometric Information Retrieval
 System Air Quality System; SEARCH - the Southeastern Aerosol Research and Characterization; GPCC -
 the Global Precipitation Climatology Centre; MODIS - the Moderate Resolution Imaging
 Spectroradiometer; IMPROVE – the Interagency Monitoring for Protected Visual Environmental; STN –
 the Speciated Trends Network. Note that IMPROVE did not contain NH₄⁺ data for 2010. “-“ indicates that
 the results of those variables not available from the WRF only simulation.

1005 **Table 3. Summary of set-up of Sensitivity Simulations**

	Run 1	Run 2	Run 3	Run 4
Emissions	2006	2010	2006	2006
Meteorological ICONs/BCONs	2006	2010	2010	2010
Chemical ICONs/BCONs	2006	2010	2010	2006

1006

1007

1008 **Table 4. Absolute and percentage differences between monthly mean of observed / satellite-**
 1009 **retrieved data and sensitivity simulations**

		Obs 2010 – Obs 2006	Run 2 – Run 1	Run 3 – Run 1	Run 4 – Run 1
Jan	CASTNET T2 (K/%)	-3.5/ -1.3	-2.0/ -0.7	-1.9/ -0.7	-1.8/ -0.7
	CASTNET SWDOWN (Wm⁻²/%)	-6.2/ -7.0	27.6/ 29.1	-0.8/ -0.9	-0.6/ -0.6
	MODIS CF (%/%)	2.7/ 4.2	1.5/ 2.3	1.4/ 2.1	1.4/ 2.1
	MODIS COT (/%)	-0.2/ -1.2	0.2/ 2.9	0.3/ 5.2	0.3/ 5.5
	MODIS AOD (/%)	-0.008/ -7.9	-0.002/ -3.9	0.008/ 15.3	0.01/ 28.0
	CASTNET Max 8-hr O₃ (ppb/%)	4.2/ 12.5	-2.9/ -9.8	-6.1/ -20.8	0.7/ 2.4
	STN PM_{2.5} (µg m⁻³/%)	-0.2/ -1.9	1.6/ 19.1	1.4/ 16.5	1.5/ 17.7
Jul	CASTNET T2 (K/%)	0.03/ 0.0	0.5/ 0.2	0.5/ 0.2	0.5/ 0.2
	CASTNET SWDOWN (Wm⁻²/%)	-2.8/ -1.1	-7.4/ -2.6	-8.9/ -3.1	-5.5/ -1.9
	MODIS CF (%/%)	1.1/ 2.0	-1.8/ -3.4	-1.8/ -3.3	-1.5/ -2.8
	MODIS COT (/%)	-0.4/ -2.7	-0.6/ -11.1	-1.0/ -17.8	-0.9/ -16.5
	MODIS AOD (/%)	-0.06/ -31.0	0.04/ 58.3	0.06/ 79.4	0.04/ 50.9
	CASTNET Max 8-hr O₃ (ppb/%)	-4.8/ -9.2	-7.6/ -15.2	-5.0/ -10.1	8.6/ 17.2
	STN PM_{2.5} (µg m⁻³/%)	-0.5/ -3.7	-0.5/ -4.5	1.5/ 14.4	1.0/ 9.8

1010

1011 **List of Figures**

1012

1013

1014 Figure 1. Comparison of seasonal plots of NMB vs NME of various meteorological variables for
1015 2006 (left column) and 2010 (right column) – T2 (temperature at 2m), SWDOWN
1016 (downward shortwave radiation), WS10 (wind speed at 10m) and Precipitation where the
1017 shapes represent different seasons (diamond – MAM, circle – JJA, triangle – SON and
1018 square – JFD) and the different colors represent different observational data (red –
1019 SEARCH, blue – CASTNET, green – NADP, black – GPCC).

1020 Figure 2. Spatial Distribution of NMB plots for JFD and JJA 2006 and 2010 for maximum 8-hr
1021 O₃ concentrations based on evaluation against CASTNET, AQS and SEARCH.

1022 Figure 3. Comparison of seasonal plots of NMB vs NME for maximum 8-hr O₃ concentrations
1023 where the different shapes represent different seasons (diamond – MAM, circle – JJA,
1024 triangle – SON and square – JFD) and the different colors represent different
1025 observational data (purple – CASTNET, black – AQS and green - SEARCH).

1026 Figure 4. Diurnal variation of T2 (top row) and hourly O₃ concentrations (bottom row) against
1027 CASTNET for JJA 2006 and 2010.

1028 Figure 5. Spatial Distribution of NMB plots for JFD and JJA 2006 and 2010 for average 24-hr
1029 PM_{2.5} concentrations based on evaluation against the IMPROVE, STN and SEARCH
1030 sites.

1031 Figure 6. Comparison of seasonal plots of NMB vs NME for average 24-hr PM_{2.5} concentrations
1032 where the different shapes represent different seasons (diamond – MAM, circle – JJA,
1033 triangle – SON and square – JFD) and the different colors represent different
1034 observational data (purple – IMPROVE, black – STN and green - SEARCH).

1035 Figure 7. Plots of annual statistics (NMB vs NME) for average 24-hr PM_{2.5} concentrations and
1036 PM_{2.5} species against different observational networks.

1037 Figure 8. Time series of Obs vs. Sim PM_{2.5}, SO₄ and NO₃ concentrations against STN for 2006
1038 and 2010.

1039 Figure 9. Scatter plots of SOA (left column) and OC (right column) concentrations at various
1040 sites.

1041 Figure 10. Comparison of soccer plots for JFD and JJA 2006 and 2010 evaluation of aerosol and
1042 cloud variables. MISR AOD, and SRB CF obs data was not available for 2010.

1043 Figure 11. Changes in hourly average surface concentrations of O₃ and PM species from 2010 to
1044 2006 (2010 – 2006).

1045 Figure 12. Changes in hourly average predictions of aerosol-cloud variables at surface from
1046 WRF/Chem simulations from 2010 to 2006 (2010 – 2006).

1047 Figure 13. Spatial difference plots for January where Run 1: 2006 baseline simulations; Run 2:
1048 2010 baseline simulations; Run 3: 2010 simulations with 2006 emissions and 2010
1049 meteorology and chemical IC/BCs; Run 4: 2010 simulations with 2006 emissions and
1050 2006 chemical IC/BCs and 2010 meteorology.

1051 Figure 14. Spatial difference plots for July where Run 1: 2006 baseline simulations; Run 2: 2010
1052 baseline simulations; Run 3: 2010 simulations with 2006 emissions and 2010
1053 meteorology and chemical IC/BCs; Run 4: 2010 simulations with 2006 emissions and
1054 2006 chemical IC/BCs and 2010 meteorology.

1055

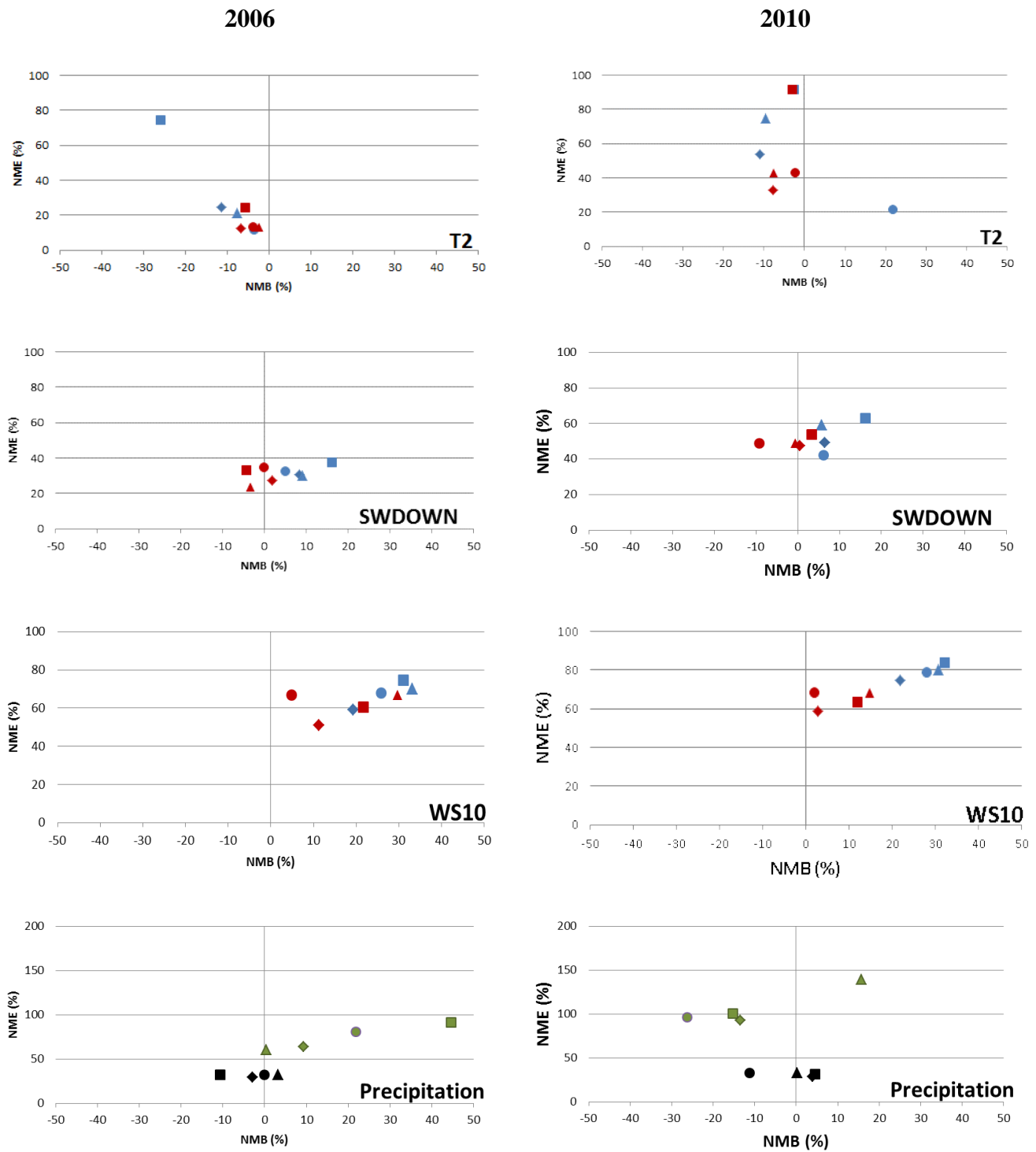


Figure 1. Comparison of seasonal plots of NMB vs NME of various meteorological variables for 2006 (left column) and 2010 (right column) – T2 (temperature at 2m), SWDOWN (downward shortwave radiation), WS10 (wind speed at 10m) and Precipitation where the shapes represent different seasons (diamond – MAM, circle – JJA, triangle – SON and square – JFD) and the different colors represent different observational data (red – SEARCH, blue – CASTNET, green – NADP, black – GPCC).

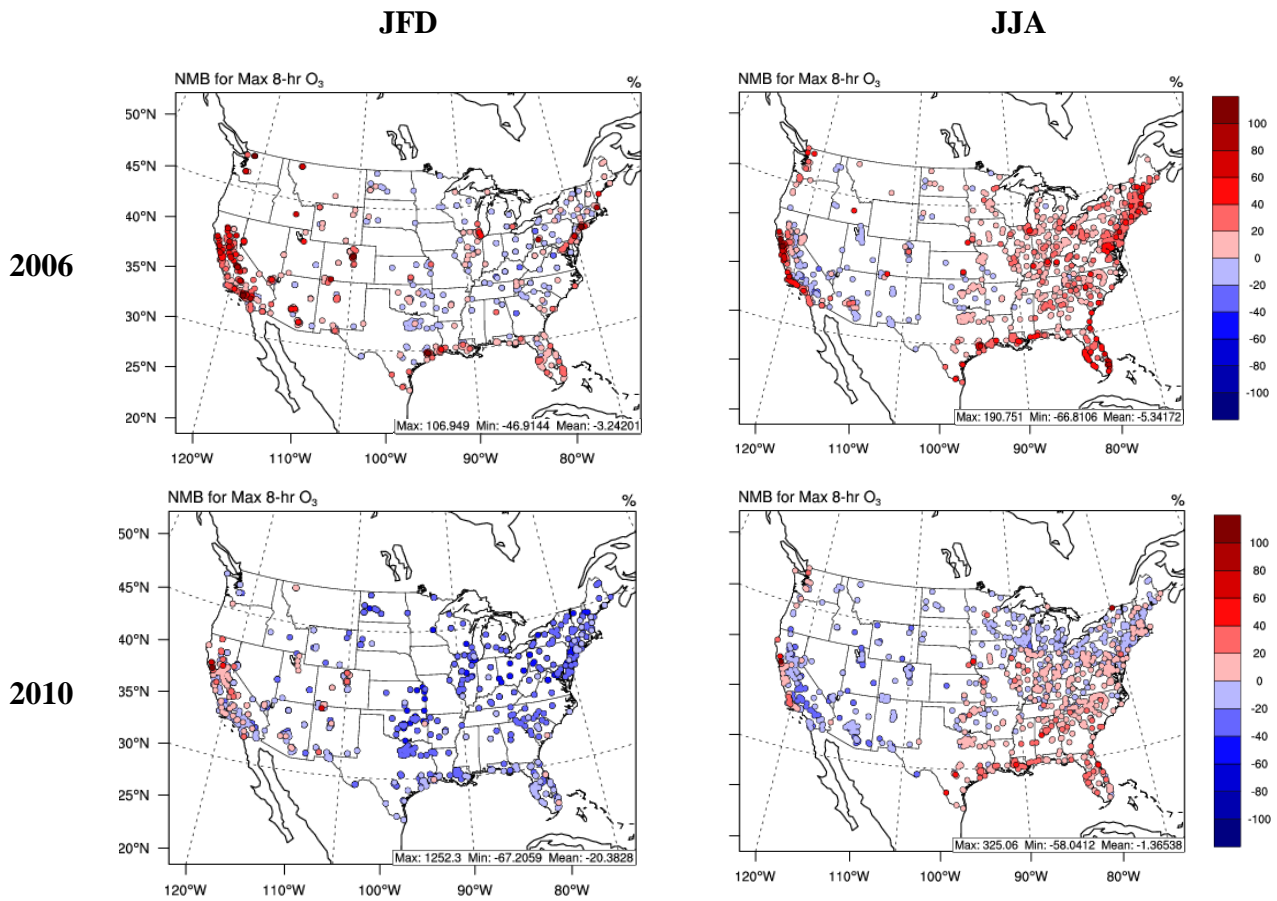


Figure 2. Spatial Distribution of NMB plots for JFD and JJA 2006 and 2010 for maximum 8-hr O₃ concentrations based on evaluation against CASTNET, AQS and SEARCH.

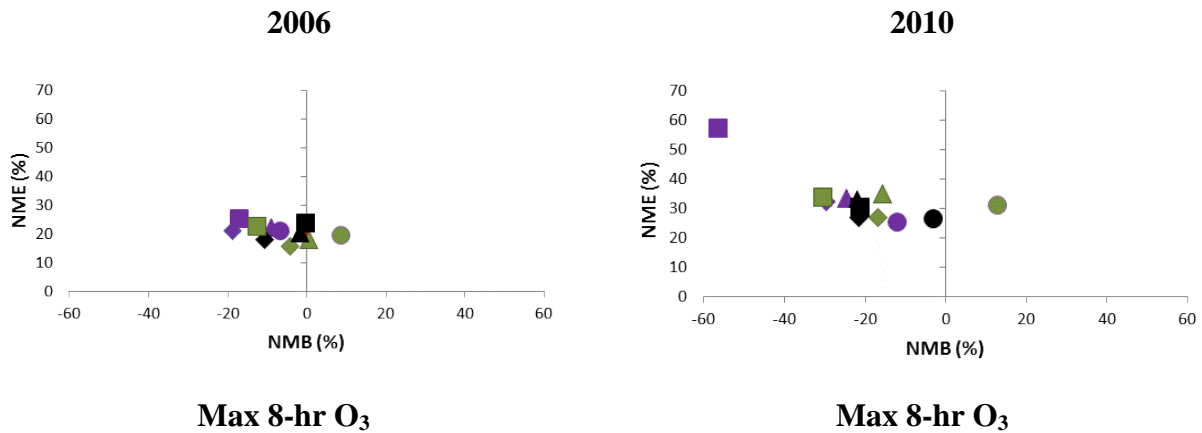


Figure 3. Comparison of seasonal plots of NMB vs NME for (a) maximum 8-hr O₃ concentrations where the different shapes represent different seasons (diamond – MAM, circle – JJA, triangle – SON and square – JFD) and the different colors represent different observational data (purple – CASTNET, black – AQS and green - SEARCH).

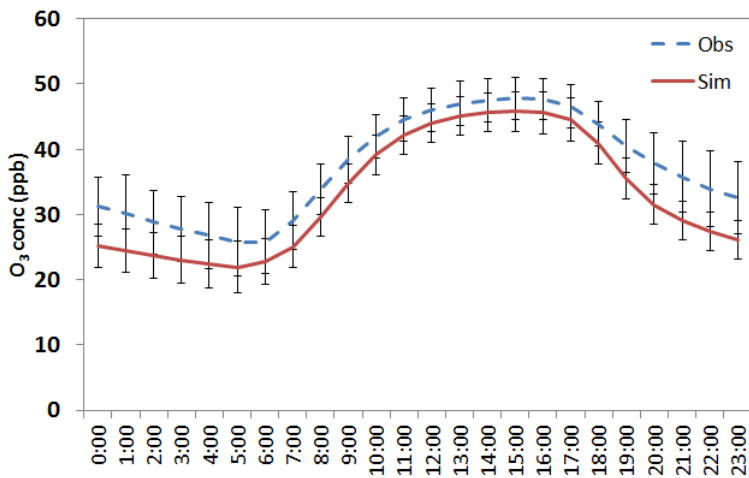
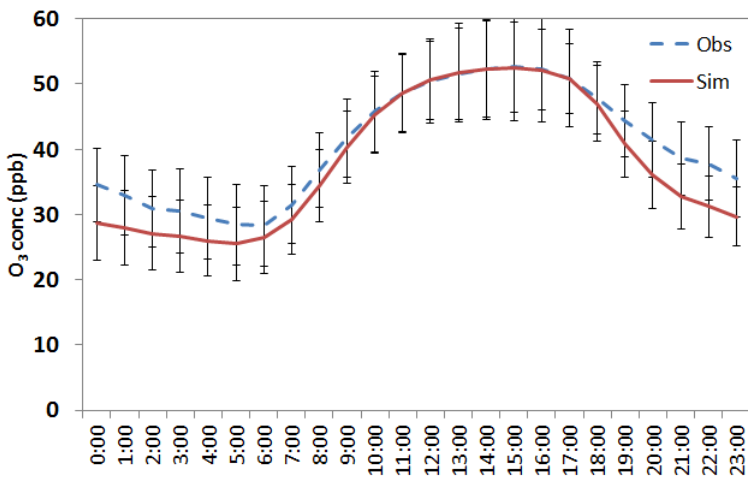
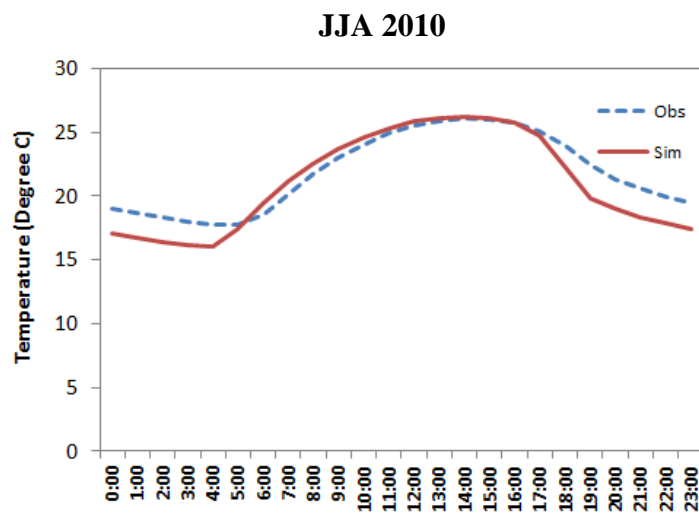
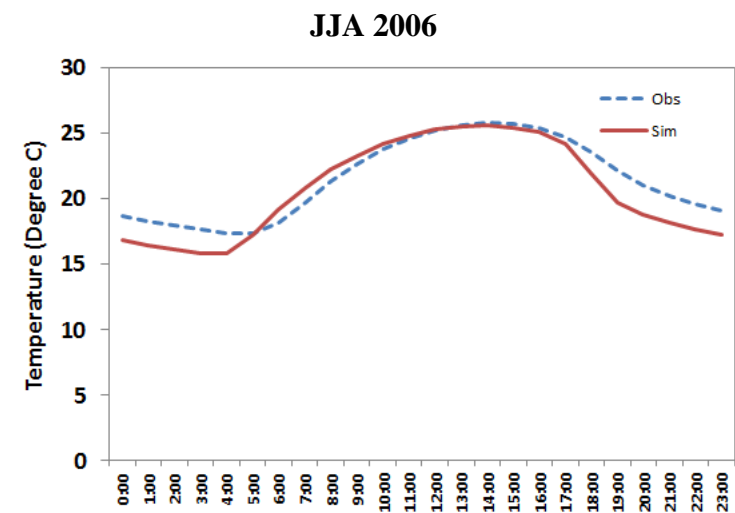


Figure 4. Diurnal variation of T2 (top row) and hourly O₃ concentrations (bottom row) against CASTNET for JJA 2006 and 2010.

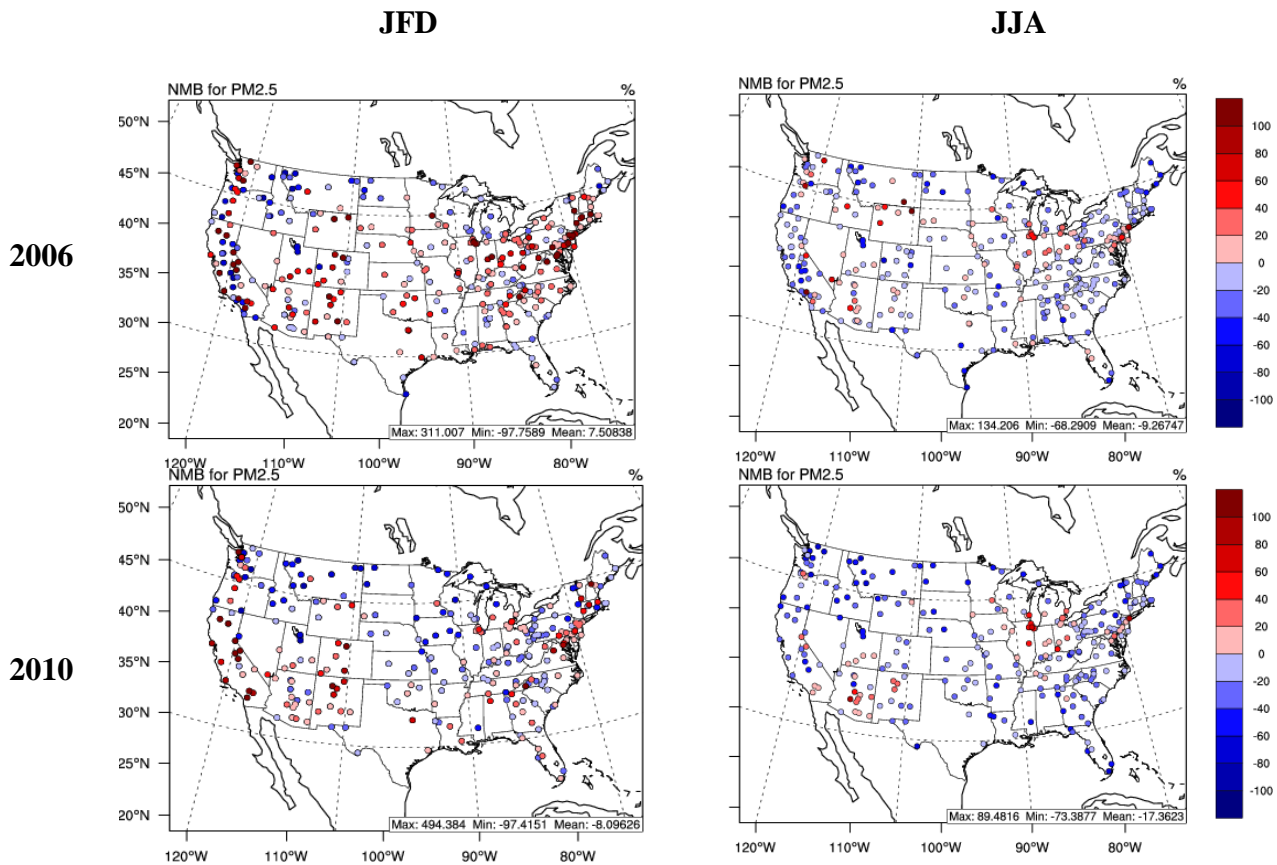


Figure 5. Spatial Distribution of NMB plots for JFD and JJA 2006 and 2010 for average 24-hr $PM_{2.5}$ concentrations based on evaluation against the IMPROVE, STN and SEARCH sites.

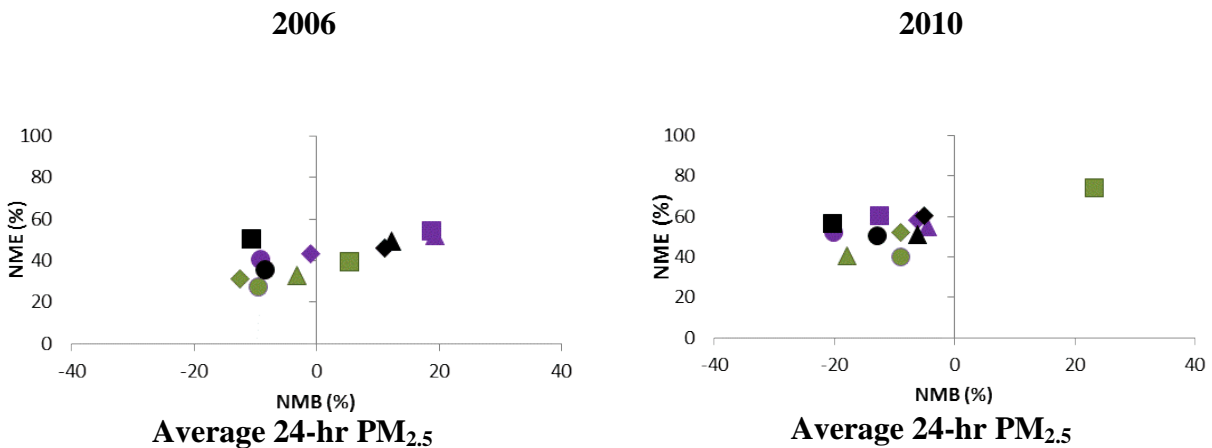


Figure 6. Comparison of seasonal plots of NMB vs NME for average 24-hr $PM_{2.5}$ concentrations where the different shapes represent different seasons (diamond – MAM, circle – JJA, triangle – SON and square – JFD) and the different colors represent different observational data (purple – IMPROVE, black – STN and green – SEARCH).

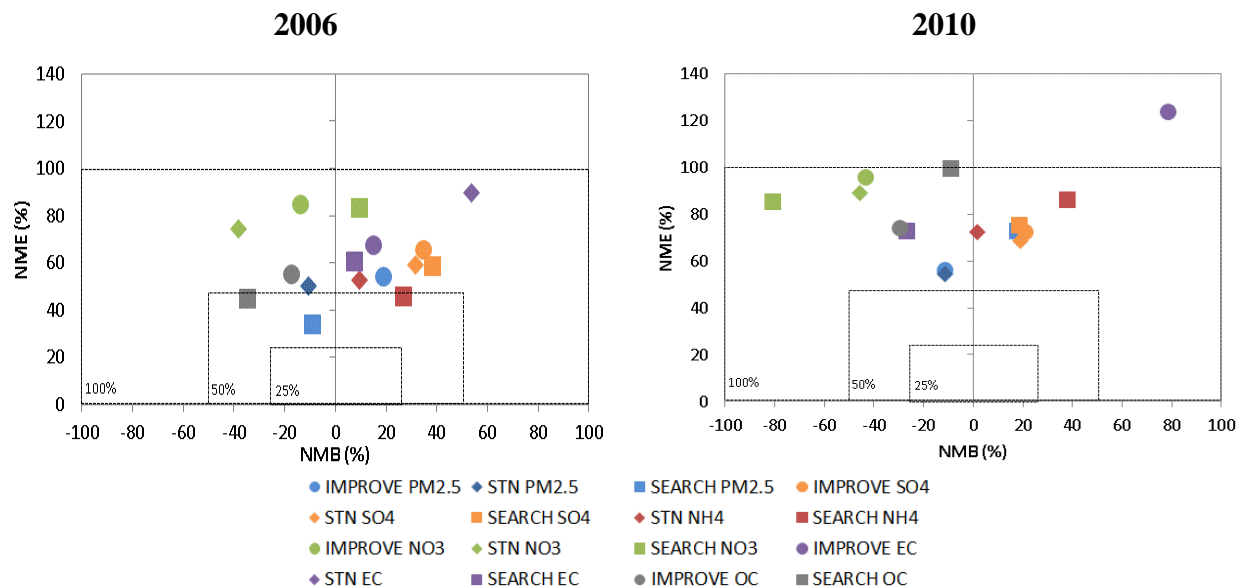


Figure 7. Plots of annual statistics (NMB vs NME) for average 24-hr $PM_{2.5}$ concentrations and $PM_{2.5}$ species against different observational networks.

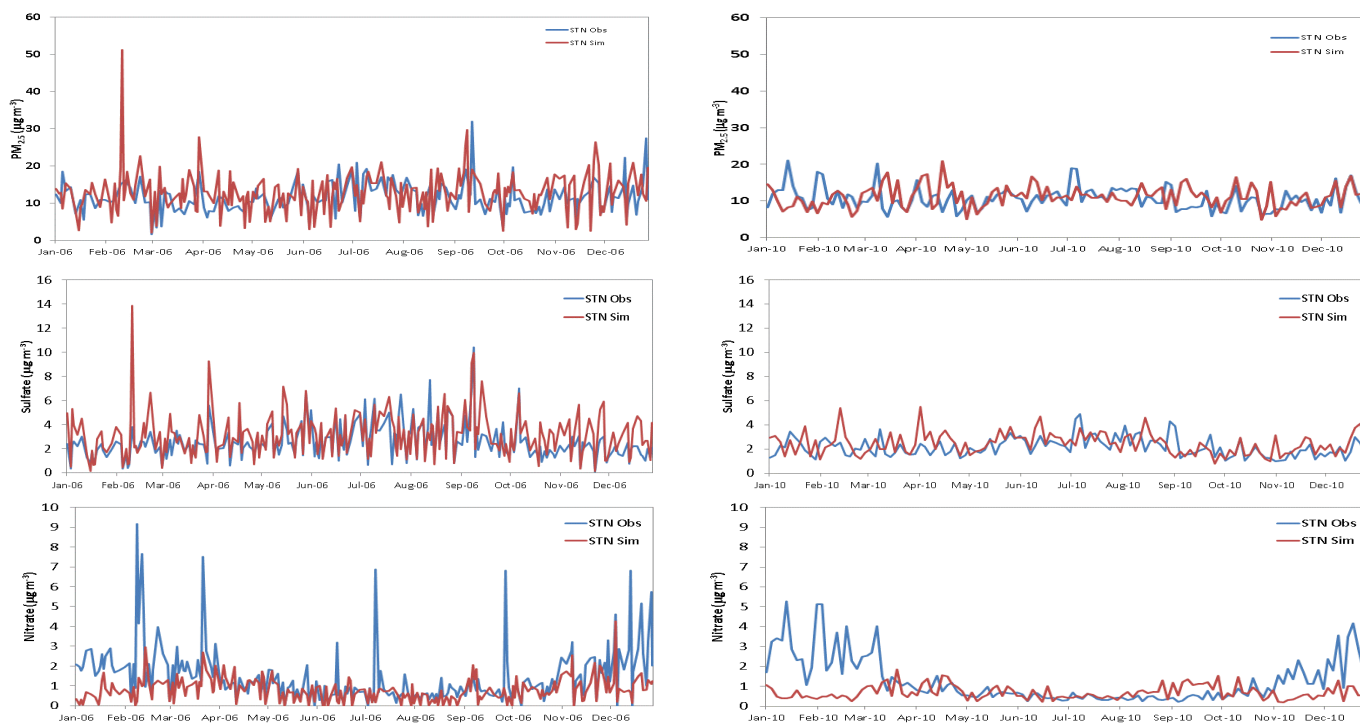
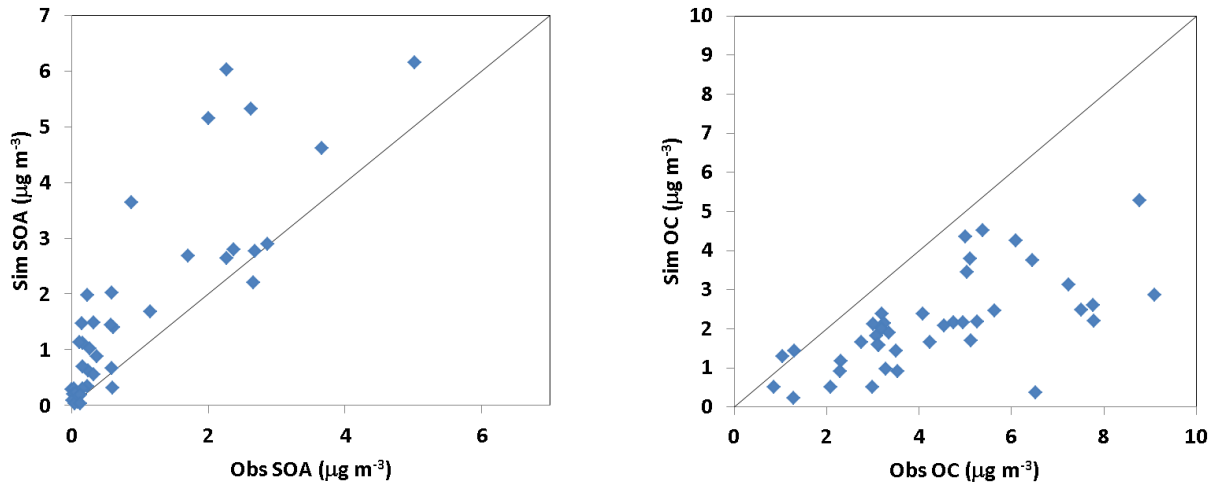
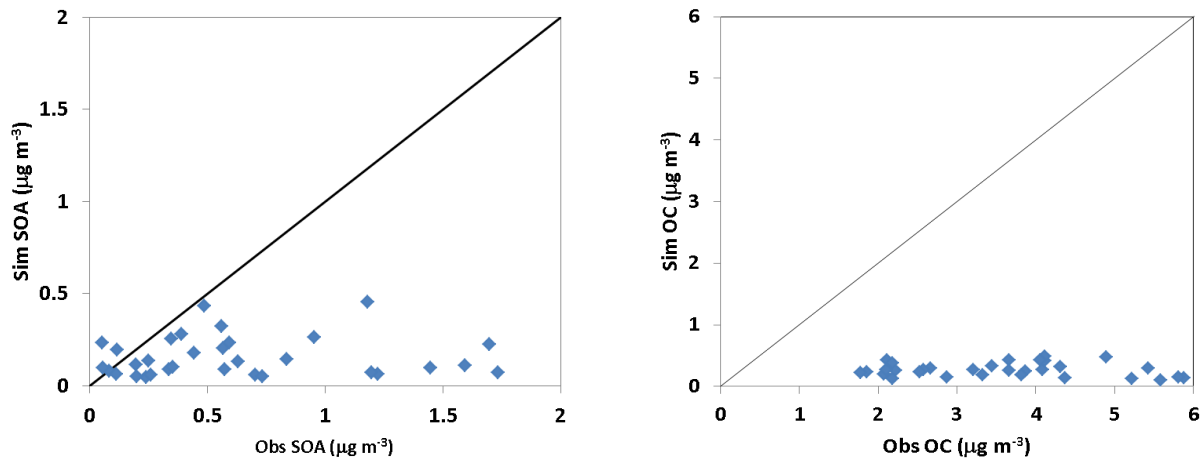


Figure 8. Time series of Obs vs. Sim $PM_{2.5}$, SO_4 and NO_3 concentrations against STN for 2006 and 2010.

Research Triangle Park, NC, Apr – Dec 2006



Pasadena, CA, May – June 2010 (this study)



Bakersfield, CA, May – June 2010 (this study)

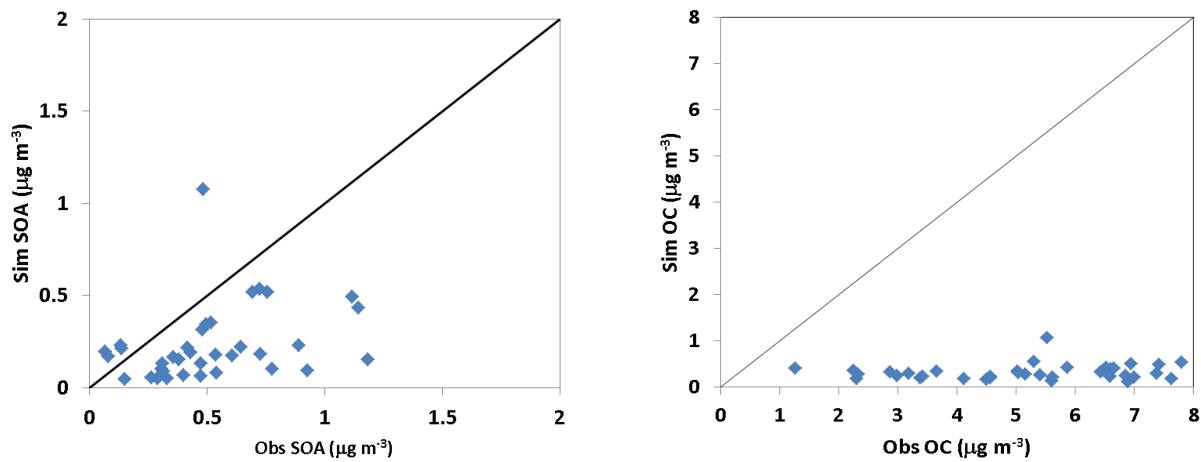
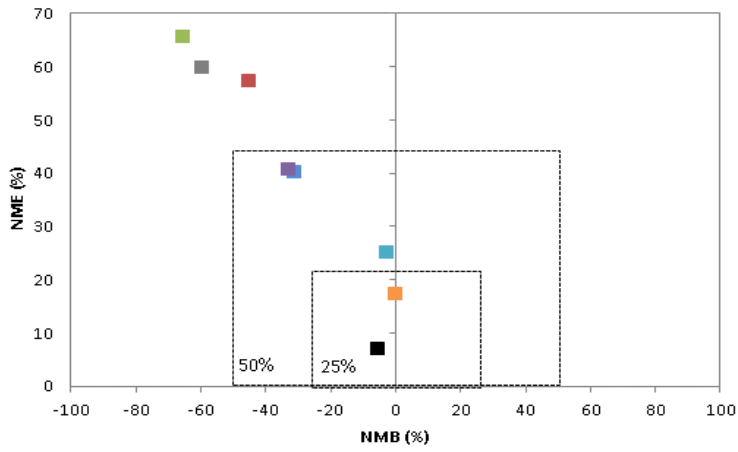
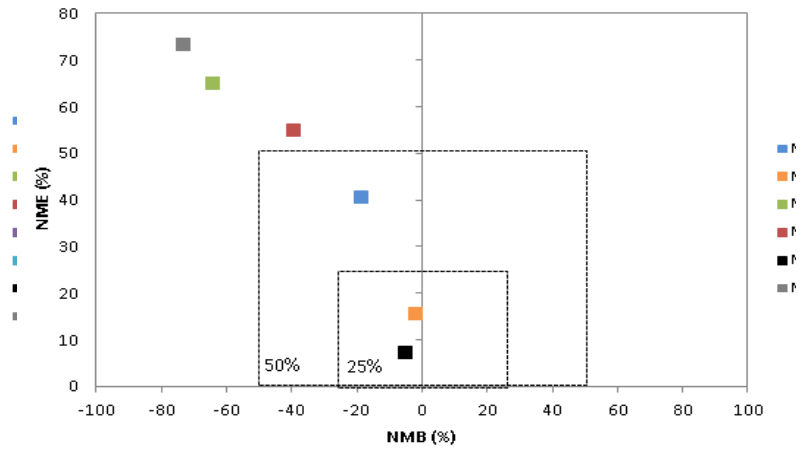


Figure 9. Scatter plots of SOA (left column) and OC (right column) concentrations at various sites

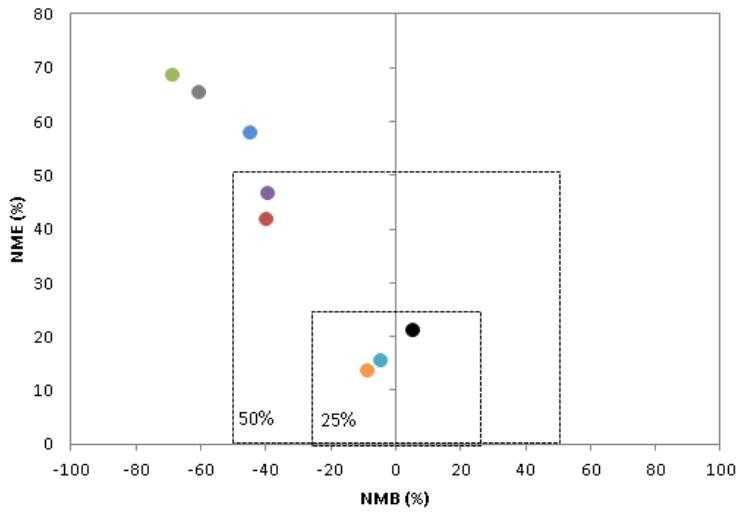
2006 JJA



2010 JJA



2006 JFD



2010 JFD

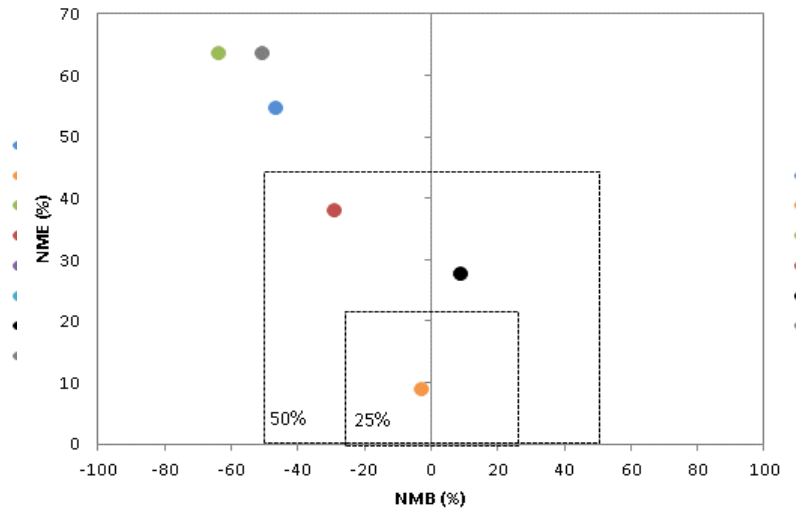


Figure 10. Comparison of soccer plots for JFD and JJA 2006 and 2010 evaluation of aerosol and cloud variables. MISR AOD, and SRB CF obs data was not available for 2010.

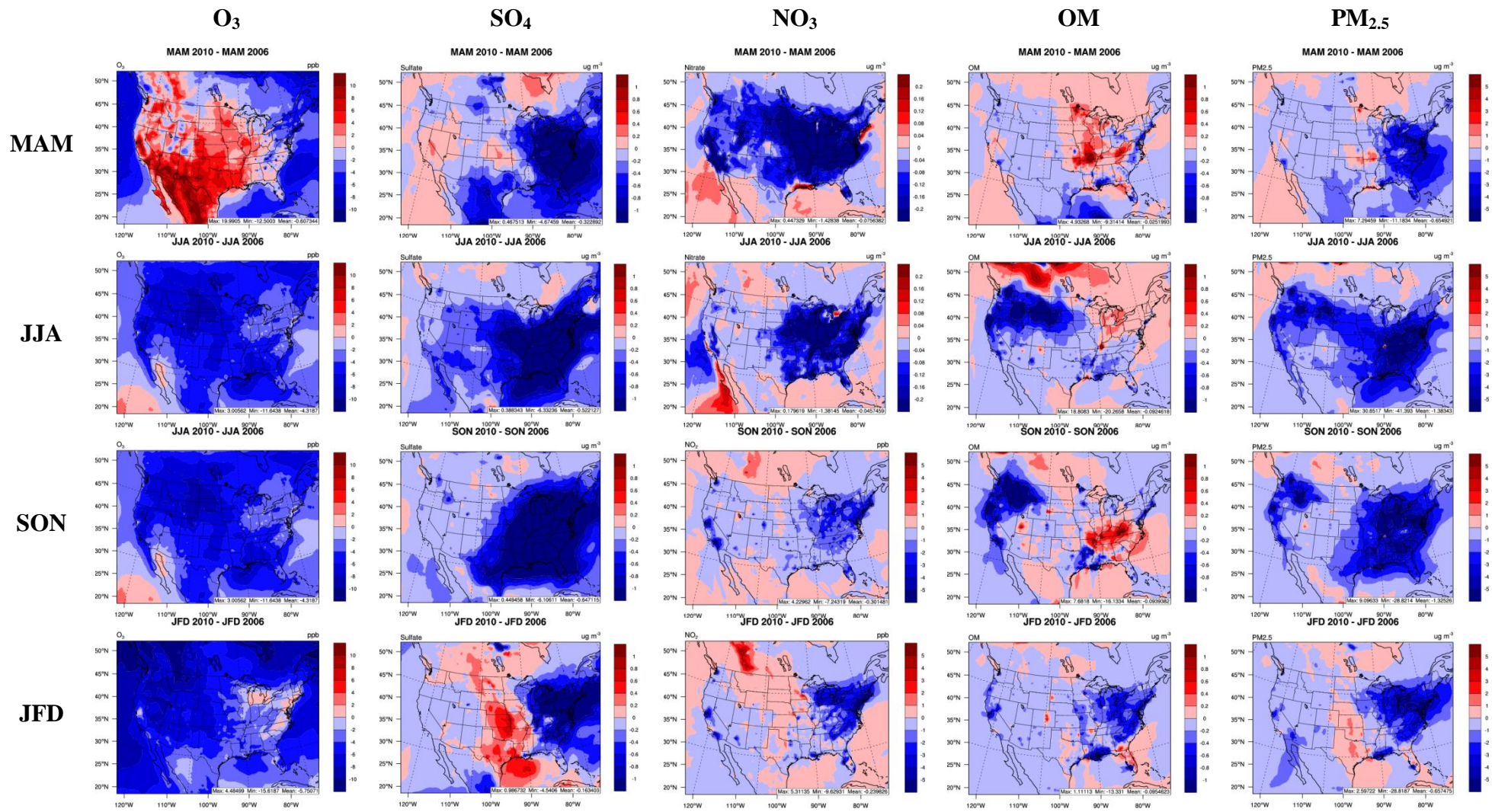


Figure 11. Changes in hourly average surface concentrations of O₃ and PM species from 2010 to 2006 (2010 – 2006).

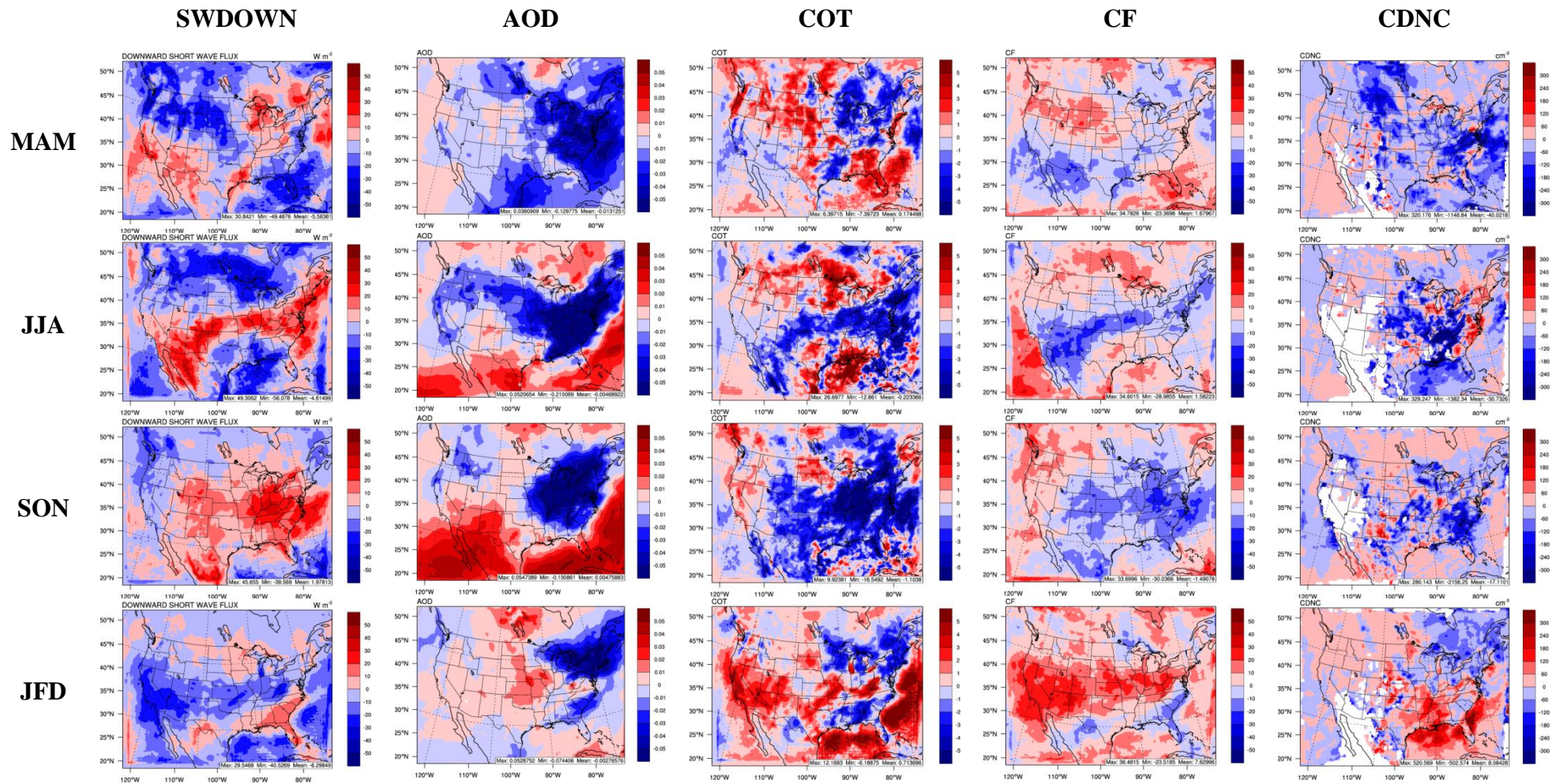


Figure 12. Changes in hourly average predictions of aerosol-cloud variables at surface from WRF/Chem simulations from 2010 to 2006 (2010 – 2006).

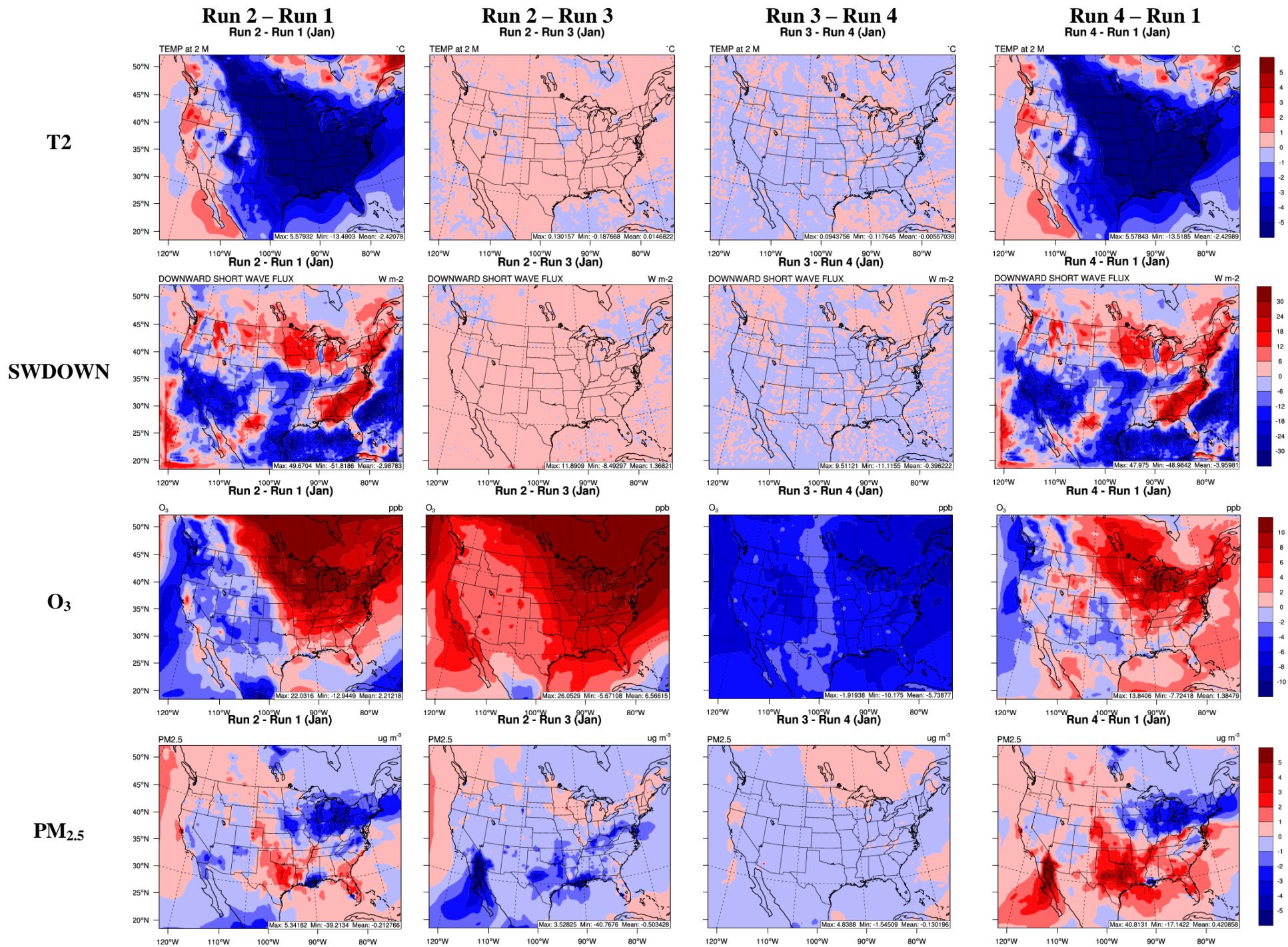


Figure 13. Spatial difference plots for January where Run 1: 2006 baseline simulations; Run 2: 2010 baseline simulations; Run 3: 2010 simulations with 2006 emissions and 2010 meteorology and chemical IC/BCs; Run 4: 2010 simulations with 2006 emissions and 2006 chemical IC/BCs and 2010 meteorology.

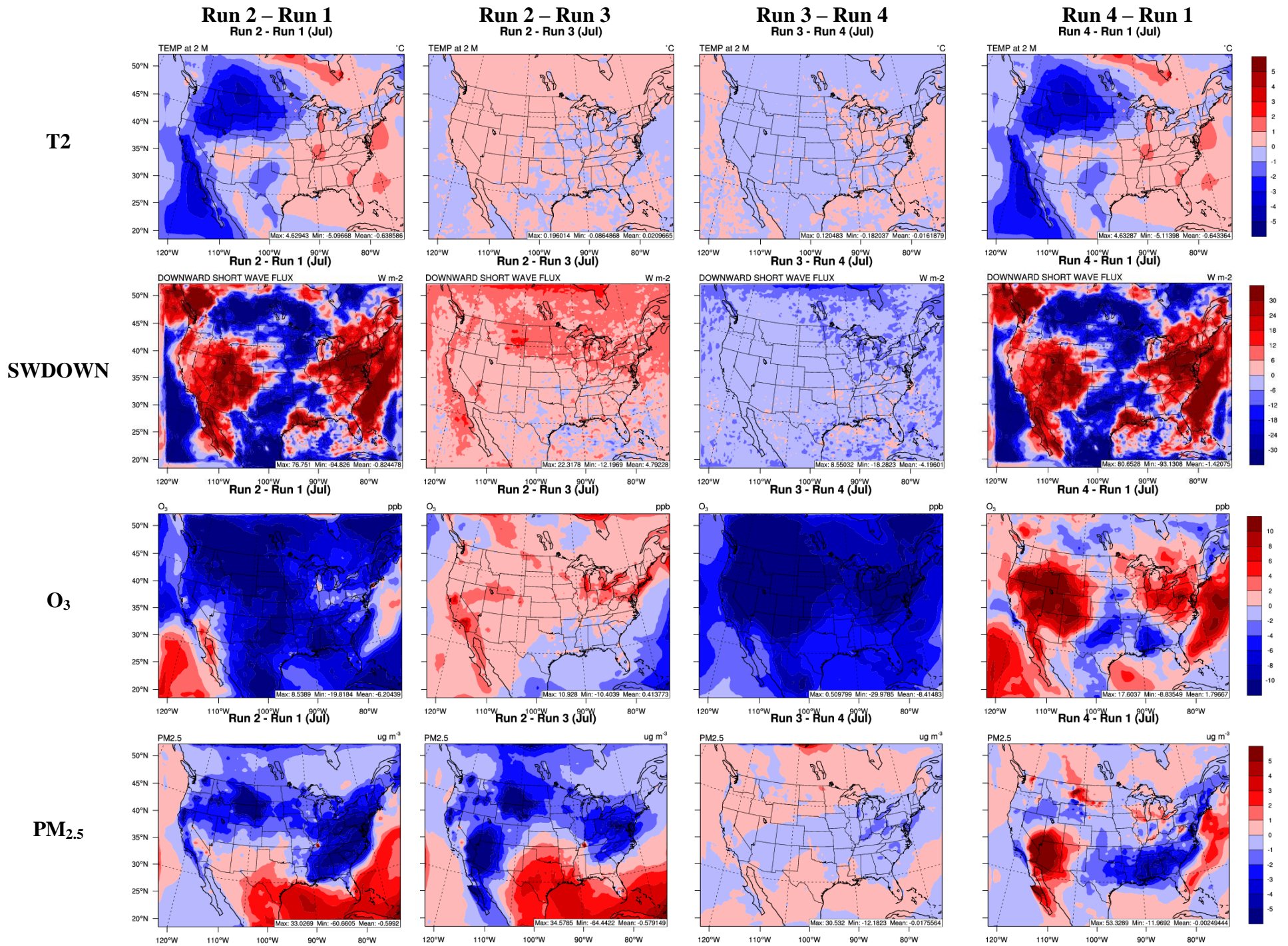


Figure 14. Spatial difference plots for July where Run 1: 2006 baseline simulations; Run 2: 2010 baseline simulations; Run 3: 2010 simulations with 2006 emissions and 2010 meteorology and chemical IC/BCs; Run 4: 2010 simulations with 2006 emissions and 2006 chemical IC/BCs and 2010 meteorology.